nature protocols

PROTOCOL

https://doi.org/10.1038/s41596-020-0354-0

Check for updates

Dynamic single-cell phenotyping of immune cells using the microfluidic platform DropMap

Yacine Bounab[1,2,13], Klaus Eyer[3,4,13], Sophie Dixneuf[5], Magda Rybczynska[3], Cécile Chauvel[5], Maxime Mistretta[1], Trang Tran[5], Nathan Aymerich[3], Guilhem Chenon[3], Jean-François Llitjos[6], Fabienne Venet[7,8], Guillaume Monneret[7,8], Iain A. Gillespie[9], Pierre Cortez[10], Virginie Moucadel[7,11], Alexandre Pachot[11], Alain Troesch[5], Philippe Leissner[5], Julien Textoris[7,11,12], Jérôme Bibette[3], Cyril Guyard[5], Jean Baudry[3]✉, Andrew D. Griffiths[2]✉ and Christophe Védrine[1]✉

Characterization of immune responses is currently hampered by the lack of systems enabling quantitative and dynamic phenotypic characterization of individual cells and, in particular, analysis of secreted proteins such as cytokines and antibodies. We recently developed a simple and robust microfluidic platform, DropMap, to measure simultaneously the kinetics of secretion and other cellular characteristics, including endocytosis activity, viability and expression of cell-surface markers, from tens of thousands of single immune cells. Single cells are compartmentalized in 50-pL droplets and analyzed using fluorescence microscopy combined with an immunoassay based on fluorescence relocation to paramagnetic nanoparticles aligned to form beadlines in a magnetic field. The protocol typically takes 8–10 h after preparation of microfluidic chips and chambers, which can be done in advance. By contrast, enzyme-linked immunospot (ELISPOT), flow cytometry, time-of-flight mass cytometry (CyTOF), and single-cell sequencing enable only end-point measurements and do not enable direct, quantitative measurement of secreted proteins. We illustrate how this system can be used to profile downregulation of tumor necrosis factor-α (TNF-α) secretion by single monocytes in septic shock patients, to study immune responses by measuring rates of cytokine secretion from single T cells, and to measure affinity of antibodies secreted by single B cells.

Introduction

The past few years have seen rapid progress of single-cell sequencing technologies in both fundamental and clinical research[1–3]. Single-cell RNA sequencing (scRNA-seq), in particular, is proving to be a powerful tool for studying gene expression at the single-cell level and for characterizing cell-type diversity[4]. Although methods such as droplet-based scRNA-seq[5] enable high-throughput analysis of tens of thousands of individual cells, measuring transcriptional profiles is not sufficient to fully assess cellular activity, because protein concentration and subcellular localization cannot be reliably inferred from mRNA expression levels[6,7]. Because proteins are implicated in most biological functions, numerous approaches have been developed to assess protein expression at the single-cell level. In particular, fluorescence-based flow cytometry[8] and CyTOF[9] allow medium-to-high-throughput single-cell phenotyping based on the detection of intracellular and cell-surface proteins, but not secreted proteins. The inability to directly detect secreted proteins can be partially alleviated by using experimental strategies such as blockage of secretion pathways[10,11], but it is not possible to tell whether the protein is secreted or stored intracellularly, nor to measure secretion rates. Fluorescence microscopy and flow cytometry enable reliable simultaneous analysis of 6–10 distinct markers, whereas CyTOF enables simultaneous detection of as many as 40 markers[9,12,13].

[1]BIOASTER Technology Research Institute, Lyon, France. [2]Laboratoire de Biochimie (LBC), École Supérieure de Physique et de Chimie Industrielles de la Ville de Paris (ESPCI Paris), Université Paris Sciences et Lettres (PSL), CNRS UMR8231, Paris, France. [3]Laboratoire de Colloïdes et Matériaux Divisés (LCMD), École Supérieure de Physique et de Chimie Industrielles de la Ville de Paris (ESPCI Paris), Université Paris Sciences et Lettres (PSL), CNRS UMR8231, Paris, France. [4]Laboratory for Functional Immune Repertoire Analysis, Institute of Pharmaceutical Sciences, D-CHAB, ETH Zürich, Zurich, Switzerland. [5]Biological Microsystems and Advanced Optics Engineering Unit, BIOASTER Technology Research Institute, Paris, France. [6]Medical Intensive Care Unit, Cochin Hospital, Paris, France. [7]EA7426—Pathophysiology of Injury-Induced Immunosuppression, Université Claude Bernard Lyon-1 - HCL - bioMérieux, Lyon, France. [8]Immunology Laboratory, Hospices Civils de Lyon, Lyon, France. [9]Value, Evidence & Outcomes, GlaxoSmithKline, Stevenage, Hertfordshire, UK. [10]R&D, Sanofi Aventis, Chilly-Mazarin, France. [11]Medical Diagnostic Discovery Department (MD3), bioMérieux S.A., Lyon, France. [12]Anesthesiology and Critical Care Medicine, Hospices Civils de Lyon (HCL), Lyon, France. [13]These authors contributed equally: Yacine Bounab, Klaus Eyer. ✉e-mail: jean.baudry@espci.fr; andrew.griffiths@espci.fr; christophe.vedrine@bioaster.org

Recently, droplet-based single-cell sequencing techniques have also been developed to quantify cell-surface proteins using antibodies labeled with oligonucleotides[7,14,15] (rather than fluorescence or mass tags), which enables simultaneous analysis of the transcriptome of the same cell[7,14]. By contrast, ELISPOT[16] has been used extensively to detect proteins secreted from individual cells. Although simple to implement, this technique is poorly quantitative. ELISPOT assays can be used to determine the frequency of secreting cells but, even then, discrimination between signals due to secretion and those due to background staining can be difficult[17,18]. Importantly, ELISPOT, flow cytometry, CyTOF, and single-cell sequencing are all based only on end-point measurements, which do not reflect the dynamic nature of cellular behavior.

Hence, a need exists for quantitative high-throughput systems that allow dynamic single-cell phenotyping, including detection of secretion rates and binding activities of both cell-surface and secreted proteins. This information is critical for the accurate analysis of immune responses that are mediated by both cell-membrane receptors and secretion of soluble factors, notably antibodies, chemokines and cytokines[19]. Deciphering dynamic processes at the single-cell level is critical to describing and understanding the fundamental mechanisms underlying immunity, to develop new and improved strategies for vaccination and cancer immunotherapy and to diagnose and treat inflammatory, autoimmune and infectious diseases.

Recently, novel technologies—based on microfabrication and microfluidics—have been developed to analyze the secretome of individual cells[20–31], some of which have been used to measure the secretion of multiple cytokines and to detect antibody secretion and antigen binding[30,31]. Compartmentalization of individual cells in picoliter-volume droplets in microfluidic systems[32,33] has also been used for high-throughput screening and sorting of antibody-secreting cells on the basis of the binding or inhibitory activity of secreted antibodies[34–36] and to analyze cellular heterogeneity in cytokine-secreting immune cells[37]. Although promising, these assays are based on only endpoint data and do not reflect the dynamic expression of immune responses.

To overcome these limitations, we recently described a simple and robust droplet microfluidic method, DropMap (Fig. 1), which we used to study the humoral immune response in mice immunized with tetanus toxoid[38]. With DropMap, single IgG-secreting cells are compartmentalized in tens of thousands of 50-pL droplets to form a stationary two-dimensional droplet array, enabling kinetic analysis by optical microscopy. A fast and ultrasensitive in-droplet immunoassay, based on fluorescence relocation to paramagnetic nanoparticles that are aligned to form beadlines in a magnetic field, enables simultaneous measurement of the IgG secretion rate and affinity for thousands of single cells in parallel. In our study, we discovered that immunization results in marked increases in the range of both single-cell secretion rates and IgG affinities, which spanned, at maximum, three and four logs, respectively[38]. We also showed differences in the dynamics of secretion rates and affinities of IgGs within and between spleen and bone marrow[38].

Here, we present a detailed step-by-step protocol for the DropMap system and describe how it can be extended to study a range of different immune cells, including B cells, T cells and monocytes, and to analyze the secretion of a variety of different proteins, such as different antibody isotypes, and a variety of murine and human cytokines (including TNF-α, IFN-γ, IL-2 and IL-6). We also describe how the measurement of secretion can be combined with the measurement of other parameters, including affinities of secreted antibodies, expression of cell-surface markers, endocytosis and cell viability. The method is rapid and sensitive, enabling, for example, the detection of secreted proteins from single cells in as little as 30 min, compared with generally >6 hours for conventional single-cell assays such as ELISPOT[16]. It is a flexible system that can be used to analyze humoral, cellular and innate immune responses. To illustrate the performance of DropMap, we describe its application to immune response analyses in a murine immunization model by measuring the secretion rate and affinity of antibodies secreted by single B cells. Importantly, from a clinical standpoint, we also show the downregulation profiles of TNF-α secretion by single monocytes obtained from septic shock patients.

Comparison with other methods

ELISPOT, flow cytometry, CyTOF and scRNA-seq are all based on endpoint measurements, which is advantageous for throughput but does not reflect the dynamic nature of cellular behavior. They do not enable the quantitative characterization of secreted proteins by living cells. Recently, commercially available technologies based on compartmentalization of cells in microfabricated chambers have been developed to perform a range of assays, including those for real-time IgG and cytokine secretion, apoptosis and cell–cell interaction[39–41]. For example, the Berkeley Lights system enables optofluidic

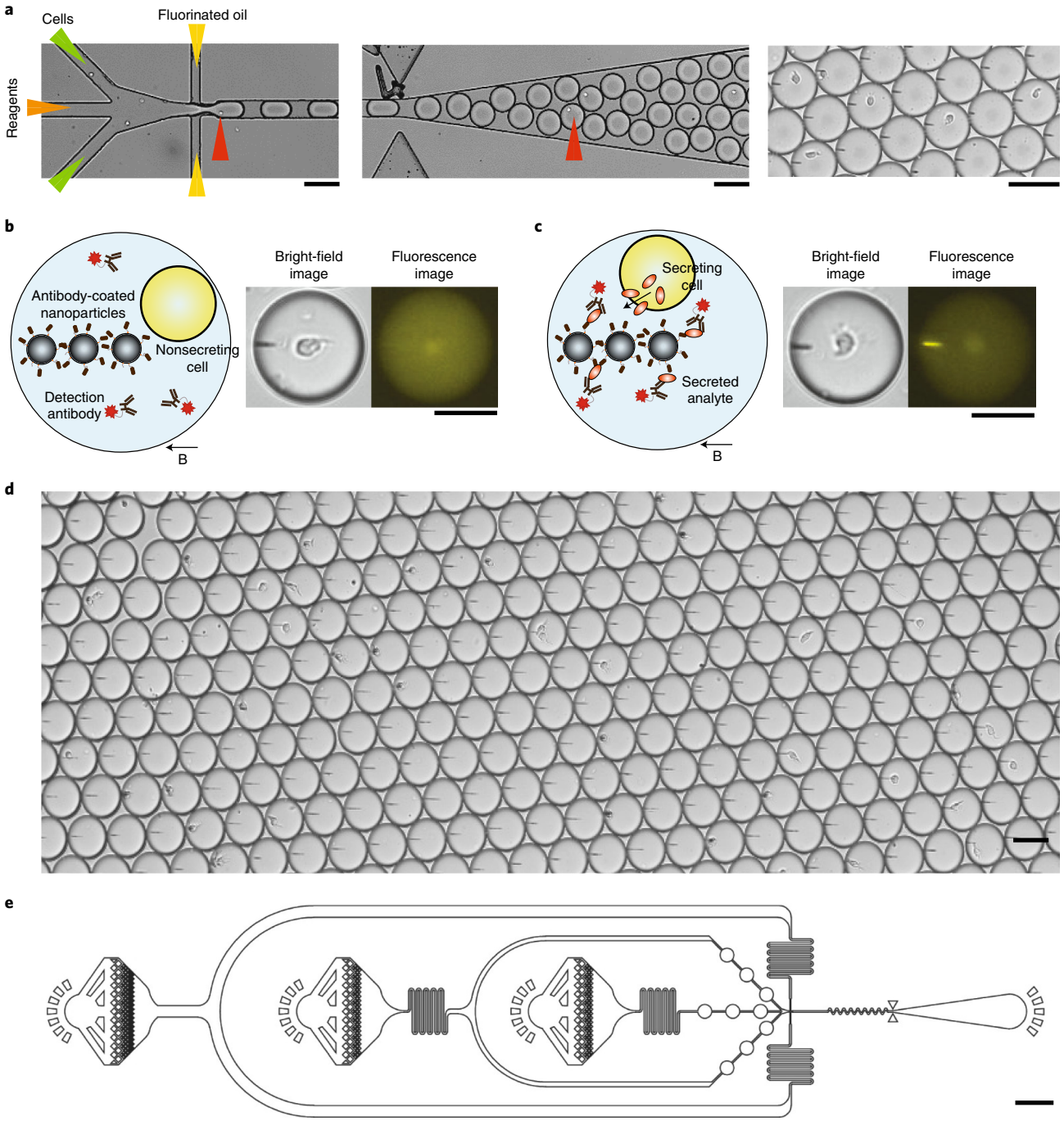

Fig. 1 | Single-cell secretion assay in microfluidic droplets. a, Co-encapsulation of cells and assay reagents into picoliter droplets. Red arrowheads show individual cells in droplets. Scale bars, 50 μm. **b**,**c**, Principle of the single-cell secretion assay in droplets. The bioassay comprises magnetic nanoparticles (300-nm diameter) functionalized with capture antibodies and fluorescently labeled detection antibodies. **b**, In the absence of secreted analyte, no binding occurs on the magnetic beadline, and the fluorescent signal remains homogeneous within the droplet. **c**, In the presence of secreted analyte, antibody-coated beads capture the secreted analyte and the fluorescent signal becomes relocalized to the beadline, owing to the fluorescently labeled detection antibody binding the captured analyte. Black arrows (labeled 'B') below the droplet indicate the direction of the magnetic field that induces beadline formation in the droplets. Scale bars, 25 μm. **d**, A bright-field image of beadlines and monocytes in a compact array of 50-pL droplets. Scale bar, 50 μm. **e**, Complete chip design used to co-encapsulate cells and reagents. Scale bar, 750 μm.

handling and analysis of single cells, including recovery of individual cells for sequence analysis, but can analyze ~10,000 cells because the system currently has 14,115 chambers ('nanopens'), whereas the DropMap system can currently analyze up to 300,000 cells. Furthermore, when used to analyze antibody secretion, the Berkeley Lights system provides only a binary (yes/no) result[41], whereas, DropMap enables simultaneous determination of both antibody secretion rate and affinity.

Other technologies using droplet microfluidics have been developed for high-throughput, single-cell, protein secretion measurement[35,37,42,43]. However, as previously mentioned, these are endpoint approaches, which do not assess the dynamic nature of a single-cell secretome. Segaliny et al.[44] used droplet microfluidics for real-time measurement of T cell activation upon recognition of target tumor cells. However, the number of droplets containing T cells and target cancer cells was low (because of Poisson statistics of cell encapsulation).

DropMap, by contrast, enables the direct measurement of protein secretion by individual living cells and the quantitative assessment of secreted proteins. Hence, using DropMap, the dynamic behavior of single-cells can be measured over time, enabling, for example, the direct and quantitative assessment of secretion rates of proteins such as antibodies, cytokines and chemokines, and, in the case of antibodies, DropMap enables simultaneous determination of both the antibody secretion rate and affinity. A DropMap chamber surface of 1 cm^2 enables the observation and analysis of 60,000 droplets, that is, ~20,000 cells over up to 12 h. Currently, the maximum number of cells we have detected simultaneously with DropMap is ~300,000 cells with a time resolution of ~21 min. The number of eukaryotic cells that can be analyzed is therefore similar to the number that can be analyzed by scRNA-seq (~10^5), ELISPOT (~10^5 per well) and the use of microfabricated nanowells (~10^5), but less than can be analyzed using flow cytometry (~10^8), CyTOF (~10^7) or droplet microfluidics with in-flow detection, where—using a similar magnetic beadline-based immunoassay—as many as 2.5 million eukaryotic cells can be analyzed per experiment[45]. The maximum number of markers that can currently be detected simultaneously with DropMap is 4, as described herein, but it should be possible to extend this to 6–10 markers, as has been done for the other systems based on epifluorescence microscopy. The use of an assay based on fluorescence relocation also negates the need for washing within the DropMap protocol.

Protocol limitations

Our protocol inherits the generic limitations of closed homogeneous fluorescence-based assays. Once immobilized, nothing can be added or extracted from the droplets without losing their identity (as defined by their position). Therefore, the immunoassay cannot be washed, no enzymes can be used for signal amplification, and multi-step assays are not possible. The immunoassay's sensitivity and range are defined by the number of added nanoparticles and the detection reagent; therefore, care should be taken when adapting the sensitivity and range of the assay to prevent excess false-positive or false-negative results (Boxes 1 and 2).

The biggest drawback of the protocol is the need for a known analyte of interest, because in the sandwich immunoassays the antibody pair is chosen according to the analyte, and the performance of the assay depends critically on the affinity and specificity of the antibodies. In addition, when assaying secreted antibodies, because purified antigens are used in the assays, cross-reactivities and/or unspecific off-target binding of the antibodies are not taken into account and need to be characterized by other methods.

Owing to the need for imaging in different fluorescence channels, care should be taken regarding optical phenomena such as pixel saturation, photobleaching and spectral overlap. Spectral overlap also limits the number of readouts that can be used to probe several cellular functions within the droplets, thus reducing the multiplexing capability as compared with CYTOF or single-cell sequencing.

Long-term studies over days are also limited because of the inability to add fresh nutrients to the cells without losing their identity. Therefore, the longest experimental time is defined by the disappearance of a critical nutrient or the accumulation of waste products in the droplets. These depend on the nature of the cells analyzed, but when using mammalian cells (Chinese hamster ovary (CHO) cells), the longest assay we have performed was 12 h. The frequency of dead cells (stained with propidium iodine) encapsulated in droplets was not significantly different from that of the reference culture in a standard CO_2 incubator over a 12-h incubation (3.2 ± 1.6% and 2.6 ± 1.6%, for droplets and the reference culture, respectively. $N = 3$, two-tailed unpaired t-test, $P = 0.67$).

Expertise needed to perform the protocol

A competent graduate student or post doc can perform the protocol. There are two critical parts of the protocol. First, the extraction and preparation of the biological sample—that is, the cells—is of great importance. These should be extracted and prepared with the least stress possible because even minor changes in the protocol might result in lower secretion rates and therefore variation in the

Box 1 | Assay setup

Choosing a pair of antibodies for the immunoassay

When choosing a new pair of antibodies to set up another immunoassay, we consider the following, ranked approaches:

1 Study literature and/or suppliers for antibody pairs that have been tested for sandwich immunoassays.
2 A neutralizing and a non-neutralizing clone will recognize different epitopes; therefore, binding interference is less likely.
3 The combination of polyclonal IgG for immobilization and monoclonal IgG for detection can also show good results, although recalibration is necessary when different batches of antibody are used.
4 Use a variety of different monoclonal antibodies and test the various combinations.

Labeled antigens and antibodies

Important points to consider when preparing the reagents for the in-droplet assay:

- Purify antibodies and antigens as much as possible. Pure reagents will allow for better results and more standardized and repeatable results.
- Be sure to remove any free dye or biotin before using the proteins in the assays. Any non-bound molecules will increase the background and reduce the sensitivity of the assay. We use several rounds centrifugation and 10,000 MWCO protein concentrators (Thermo Scientific/Pierce) to remove free dyes.
- When labeling the antigen with biotin or fluorescent dye, use a random method to conserve all available epitopes on the antigen.
- Do not overlabel proteins. We aim for a degree of labeling (molecules/protein) of around 2. Overlabeled antigens will not enable sensitive immunoassays.
- After labeling and purification, determine the exact concentration of the protein because the bioassay performance varies greatly with concentration.
- Test the labeled proteins in an ELISA format to determine the absence of interference. For antigens, we usually assay this by ELISA. Coat the labeled and unlabeled antigen on the ELISA plate (separately) and add the antibody in varying concentrations. Compare the two binding curves.

Set up concentration range

The in-droplet assay enables a wide range of measurements. The assay can be set up to be very sensitive (LOD of 500 molecules) or to span a wider concentration range. Use bulk measurements that help set up single-cell measurements. Look for literature values for bulk measurements that indicate the number of cells, time, volume and concentrations of the experiment to estimate the secretion rate. This crude estimation can serve as a starting point for assay setup.

When setting up the assay, four factors determine its performance: concentration of beads, immobilization reagent, detection reagent and the apparent dissociation constants of the used antibodies for capture and detection. For starting values, refer to the table below.

Parameter	No. of nanoparticles	Immobilization antibody	Labeled detection antibody	Apparent dissociation constant of capture and detection antibodies
Influence on capacity of the beads[a]	+++	+++	−	−
Influence on sensitivity[a]	+	+++	+++	++
Influence on measurement range[a]	++	++	++	+
Use of too much will result in…	Plateau in the calibration curve. Great for yes/no answers; less suitable to quantify secretion rates	Increased waste	Decreased sensitivity; increased LOD	NA
Use of too little…	Absence of beadline; no reliable measurement of relocation	Plateau in the calibration curve. Great for yes/no answers; less suitable to quantify secretion rates	Lower relocation values	NA
Use of well-balanced amounts	Binding capacity matches the quantity of labeled detection reagent	Calculated as 1–2× capacity of the beads (minimized waste)	Matches capacity of beadline	As high affinity as possible
Starting point for 0.1–10 molecules/s (0.5 h assay time)	170 beads (in-droplet dilution of a factor of 50 from stock)	34 µmol per milligram of beads	0.8 nmol/l	As high affinity as possible
Starting point for 10–1,000 molecules/s (0.5 h assay time)	1,200 beads (in-droplet dilution of a factor of4 from stock)	75 nmol/l per droplet	75 nmol/l (30 nmol/l for antigen)	As high affinity as possible

[a]The magnitude of the effect is indicated: +++, strong; ++, medium; +, weak; −, no effect.

results. The work with human and animal samples needs to be performed by properly trained and skilled experimenters, with appropriate safety precautions and with ethical approval where necessary, and in accordance with local legislation. Second, the proper preparation of the chamber and droplets is critical to eliminating or restricting droplet movement over time and improving data quality and the reliability of the process, but a researcher from any discipline can easily become proficient in the procedure.

Experimental design

The DropMap protocol is based on compartmentalization of single cells in tens of thousands of 50-pL droplets that are immobilized in two-dimensional droplet arrays and analyzed by fluorescence microscopy[38] (Fig. 1). The droplets can therefore be monitored over time and cellular dynamics can

Box 2 | Extraction of parameters

Limit of detection. This requires a calibration curve, a negative sample (e.g., cells not producing the analyte) and a positive sample (e.g., cells producing the analyte).
First, you will have to define a limit of detection (LOD) for the extracted secretion rate. Below this value, you will not be able to determine whether a cell secretes the analyte. To set up the LOD, we recommend that you have a calibration curve, a negative sample and a sample (such as a cell line) with positive events. Use the data from the calibration curve to set various thresholds and use them on the negative and positive samples to quantify the number of false positives and false negatives, given a certain threshold. As a starting point, we use the definition of the LOD by Armbruster and Pry[46], which states:

$$Limit\ of\ detection(LOD) = \overline{x_{blank}} + 1.645 \times \sigma_{blank} + 1.645 \times \sigma_{low}$$

where x_{blank} is the mean fluorescence relocation in a negative sample, σ_{blank} its standard deviation and σ_{low} the standard deviation of a sample with low concentration. If this threshold is too low, you will include mostly false-positive events (visible by an increased number of events in the negative sample), whereas a too-high threshold increases false negatives (a decreased number of events in the positive sample). If the analytical resolution is too low, set up the assay anew with different antibodies or concentration ranges (Box 1) and repeat the experiments.

▲ **CRITICAL** Good labeling and high signals will decrease the LOD and decrease the frequency of false positives and negatives.
Number of cells. Droplets with living cells are automatically detected in the analytical pathway. It is important to have a low mean number of cells per droplet ($\lambda < 0.2$) and an absence of cell clusters.
Secretion rates. This requires a calibration curve and data measured over time.
Your calibration curve will consist of an increasing phase of fluorescence relocation, a plateau and an ensuing decreasing phase, due the Hook effect (see Fig. 3b,e). Present in one-step immunoassays, the Hook effect leads to a decrease in signal at high analyte concentrations. In our case, at analyte concentrations higher than beadline capacity, the non-bound analyte competes with the bound analyte for the detection reagent, and the measured fluorescence relocation decreases. Therefore, take care to use only the increasing phase for calculations of secretion rates in the cell measurements. Use the fitting parameters from the calibration curve to convert the measured in-droplet fluorescence relocation into concentration. The secretion rate is then simply calculated by the change of concentration over time. For each droplet followed over time, we can therefore define:

$$Secretion\ rate\left[\frac{molecules}{s}\right] = \left(\frac{1}{n-1}\left(\sum_{1}^{n-1}\frac{c_{i+1}-c_i}{\Delta t}\right)\right) \times N_A \times V \quad (1)$$

with n as the number of time points, c as the concentration present in the droplet at each time (i) (in picomoles; according to the calibration curve), Δt as the time difference between two measurement points, N_A as the Avogadro constant and V as the volume of the droplet (in picoliters).
Extraction of affinity (IgG assay). In addition, when a fluorescent variant of the antigen of interest is introduced into the assay, affinity of the secreted antibodies can be assayed (for more information, see ref. [38]). The ratio of relocated antigen fluorescence onto the beadline and free antigen within the droplet can be used to calculate the strength of the interaction (K_D) once the concentration of antibody is known. This concentration is accessible using calibration curves (see 'Secretion rates' above). If the secreted IgG recognizes the antigen, the ratio of fluorescent antigen bound to IgG on the beadline and mean fluorescence within the droplet can be used to calculate the strength of the interaction (K_D). The K_D is determined from the slope of the line defined by plotting the relocation of fluorescent anti-IgG F(ab')2 (concentration dependent) against the relocation of fluorescent antigen to the beadline at different concentrations of IgG below the maximum capacity of the beadline (≤50 nM, concentration and affinity dependent).

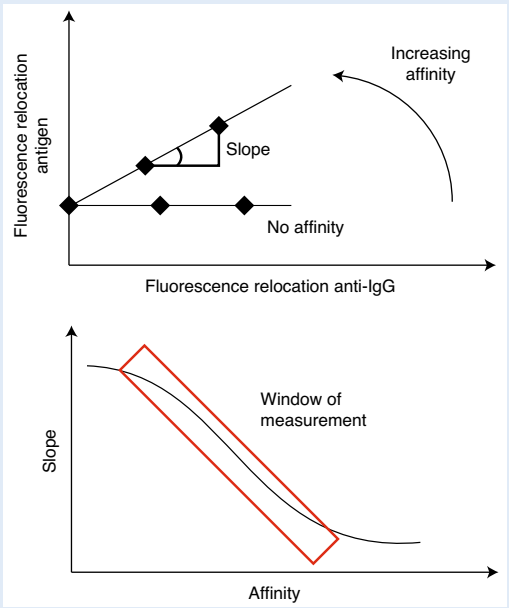

Measurement of murine IgG affinity. Relocation of fluorescent antigen and fluorescent anti-IgG detection antibody are determined by dividing the fluorescence intensity measured on the magnetic beadline (I_B) by the background fluorescence of the droplet (I_D). To calculate K_D, antigen relocation (I_B/I_D antigen) is plotted against anti-IgG detection antibody relocation (I_B/I_D anti-IgG). The slope of this plot increases with increasing

Box 2 | Extraction of parameters (Continued)

affinity; that is, decreasing K_D. The use of several antibodies with different, but known, affinities (measured, e.g., using surface plasmon resonance) enables calibration of the slope to determine K_D.

Slopes of several antibodies with known affinity against the antigen are needed to calibrate the assay. We determined the slopes for a panel of seven purified anti-tetanus toxoid IgGs with affinities ranging from 300 to 0.02 nM in our initial study[38] and have since reproduced this curve using a variety of different antigens. If the antigen is multimeric, or epitopes are present more than once, an apparent dissociation constant will be measured instead of K_D.

Be aware that the slopes for different isotypes (e.g., IgG1 and IgG2) will need different calibration curves because of their differences in fluorescence relocation[38]. If the slope is <0.03, no affinity can be detected. If the slope is >1; K_D is at or <0.1 nM but cannot be resolved any further.

To validate the antigen and antibodies, and to make sure that the calibration curve can be used for the system of interest, we assay 2–3 antibodies with known but different affinity and use the slope to calculate the K_D. The K_D should be compared with the K_D measured using an independent method, such as surface plasmon resonance.

be captured by taking images at regular intervals. Compartmentalization of single cells in droplets enables the measurement of secreted molecules, which remain in the droplets, in combination with measurement of cell-surface markers and other phenotypic characteristics. Secreted molecules are quantified using a fluorescence relocation–based sandwich immunoassay. A capture antibody is used to capture the analytes on antibody-coated paramagnetic nanoparticles within the droplets. These nanoparticles are aligned to form a beadline by applying a magnetic field, and the captured analytes are quantified by measuring relocation of a fluorescently labeled detection antibody to the beadline. The protocol consists of six major stages, as detailed in the following sections.

Microfabrication of the droplet production chip (Steps 1–22)

Microfluidic chips for droplet production are fabricated in poly(dimethysiloxane) (PDMS) using soft-lithography[47] as described previously[35]. Droplet makers are commercially available from a variety of commercial suppliers, as an alternative for laboratories without the necessary equipment and facilities to perform these steps. The droplet production chip is designed to produce monodisperse 50-pL droplets using hydrodynamic flow focusing[48] and contains three inlets to introduce (i) the fluorinated carrier oil containing fluorosurfactant, (ii) the suspension of cells and (iii) the assay reagents (functionalized nanobeads, labeled detection probes, a live/dead cell probe, and others), as well as one outlet for collecting the produced droplets[35] (Fig. 1d; see Supplementary Data 1 for the complete chip design CAD file).

Microfabrication of the droplet incubation chamber (Steps 23–30)

The immobilization and storage of aqueous droplets in a 2D array is the core of the DropMap approach. Immobilization of the droplets enables time-course measurements of droplet-based biological assays[49–54]. Because the height of the chamber is less than the droplet diameter, the observation chamber is able to immobilize 50-pL droplets. Incubations and observations over time are therefore made possible for short to medium time ranges (5 min to 24 h) at temperatures between 4 °C and 37 °C.

We use a simple, cost-effective and reproducible method based on double-sided tape and two standard microscope slides (75 mm × 25 mm × 1 mm) to fabricate the droplet incubation device (Fig. 2, see Supplementary Data 2 and 3 for the masks for the double-sided tape used to prepare the observation chamber and for laser ablation). The fabrication method is flexible, and customized microfluidic chambers can be fabricated, depending on the droplet volume and the number of droplets to be analyzed: several types of double-sided adhesive tape with different thicknesses are commercially available (e.g., from 3M), and any observation chamber shape and size can be made by cutting the tape with a plotter. The use of glass results in an optically transparent system, whereas the double-sided tapes used adheres strongly and stably to the glass surfaces, preventing fluid leakage and evaporation. Last, after the experiments the chamber can be cleaned and reused several times. To do so, clean the outer surfaces with ethanol or isopropanol and flush the chamber with pure fluorinated oil to remove droplets.

Functionalization of nanoparticles (Step 31A/31B)

Another important key feature of our droplet-based immunoassay is the use of many paramagnetic nanoparticles per droplet (Box 3). Magnetic nanoparticles are well suited to immunodetection technologies, owing to their large surface-to-volume ratio, monodispersity, stability and ease of manipulation in a magnetic field. Compared with approaches relying on the co-encapsulation of a

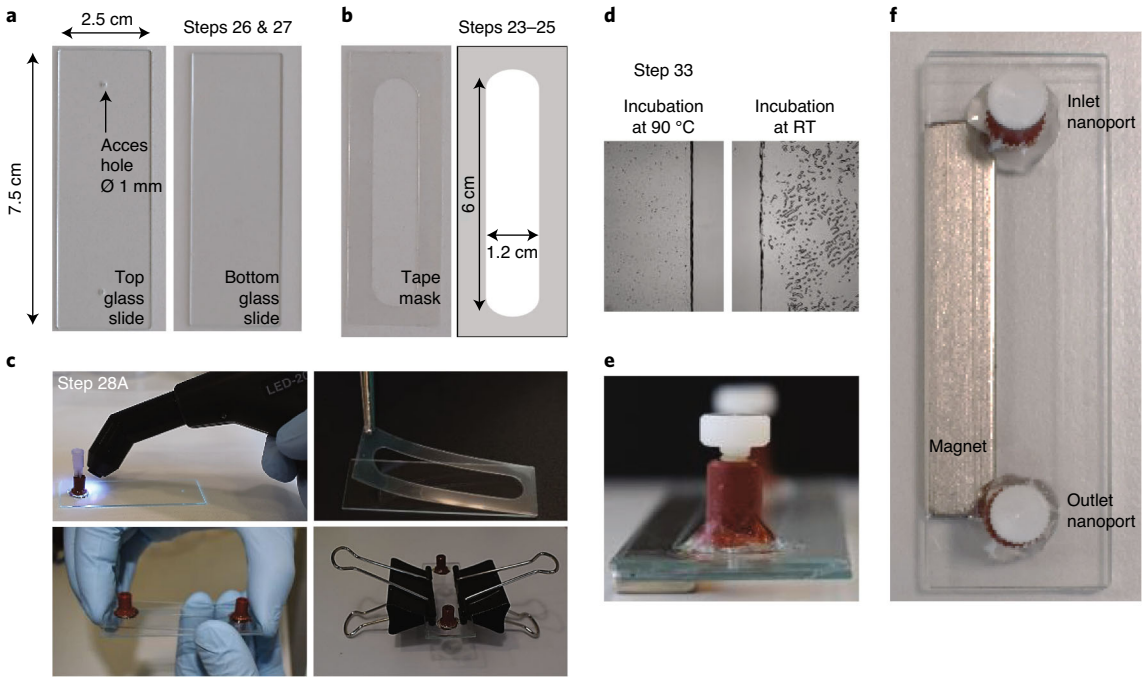

Fig. 2 | Fabrication of the microfluidic glass chamber using double-sided adhesive tape. a, Dimensions of the upper and lower glass slides enclosing the chamber. The upper slide contains two 1-mm-wide holes. Droplets are injected through one hole (the other one acts as a vent). **b**, Dimensions of the adhesive tape and pattern of the chamber. **c**, Key steps for droplet chamber fabrication. **d**, Bright-field images of the glass/tap composite: Saffman-Taylor fingers are formed at room temperature (RT); they are not formed after a 90 °C incubation (Step 28A(vi)). **e**,**f**, Device composition: two glass slides (at bottom and top) sealed with double-sided adhesive tape: (**e**) two inlet/outlet nanoports (in the top glass slide, sealed with two caps) and (**f**) a magnet glued to the bottom glass slide.

Box 3 | Distribution of cells and nanoparticles per droplet

Cells. In the absence of cell clusters (i.e., the cells are well individualized and suspended), the cellular loading in this protocol follows a Poisson distribution, which is a special case of the binomial distribution. The mean number of cells per droplet, λ, is determined by the number of cells in the initial solution and the volume of an individual droplet (see the table below, 50-pL droplets). Although a higher λ will increase the throughput and might be advantageous to increase the number of low-frequency events, a lower λ is preferable for single-cell measurements. A higher λ will increase the frequency of droplets containing multiple cells, and data analysis needs to be adapted to cope with these events. We usually aim for a λ of ~0.2–0.3, which is a compromise between maximizing the frequency of droplets with one cell and minimizing the frequency of with multiple cells (see the table below). We recommend validating the λ for each experiment by counting the number of cells in a subset of droplets (e.g., 50 droplets) because it will also be needed to calculate the total number of cells, and the frequency of positive events (see Box 2).

Cells per ml (million/ml)	λ	Empty droplet (%)	Droplets with a single cell (%)	Droplets with multiple cells (%)
5	0.1	90	9.5	0.5
10	0.2	78	19	3
20	0.4	67	27	6

Nanoparticles. An advantage of the protocol described here is the co-encapsulation of single cells with multiple nanoparticles instead of the co-encapsulation of a single cell and a single microparticle[35,36]. With a homogeneous suspension of nanoparticles and a mean, λ, of hundreds to thousands of nanoparticles per droplet, the distribution is binomial. For the two conditions presented here (170 and 1,200 nanoparticles per droplet), the standard deviations are 7 and 17, respectively, and the coefficient of variance (CV) is <0.05. Therefore, every droplet contains approximately the same number of nanoparticles, and the low CV ensures that drop-to-drop variation has a minimal impact on the results. If droplets with no beads are present during analysis, these probably stem from errors in the flow ratios during encapsulation that are due, for example, to the presence of clusters of beads or cells, dust in the microfluidic chips or operating errors.

single cell and a single microparticle[35], the use of nanoparticles increases the binding capacity and lowers the number of droplets containing no particles, which improves the performance of the assay. The protocol has been optimized so that, once a strong magnetic field is applied, each droplet contains a single, homogeneous, elongated aggregate of hundreds of nanoparticles, which appears in bright-field images as a horizontal dark beadline located within the droplet (Figs. 1, 3). The number of

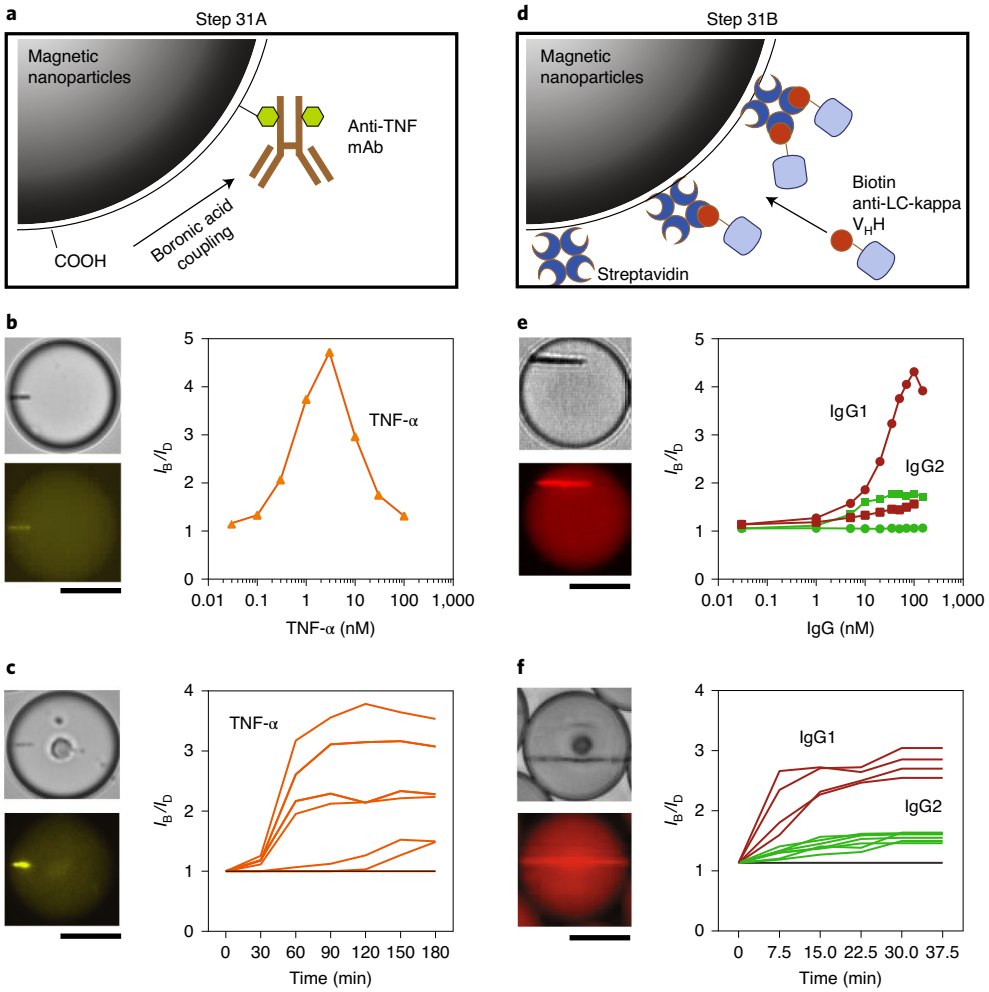

Fig. 3 | Characterization of functionalized nanoparticles in droplets. a, Schematic representation of nanoparticle coating for TNF-α detection. The bioassay comprises paramagnetic nanobeads functionalized with anti-TNF-α antibodies using boronic acid coupling to glycosyl groups. **b**, Detection of human recombinant TNF-α in 50-pL droplets. The relocation of the fluorescently labeled detection antibodies in the presence of different concentrations of TNF-α. The signal was determined by dividing the fluorescence intensity measured on the magnetic beadline (I_B) by the background fluorescence of the droplet (I_D). Top left, bright-field image. Bottom left, fluorescence image. Right, signal (I_B/I_D) as a function of TNF-α concentration. **c**, Time courses of TNF-α secretion by individual monocytes. Each curve represents the kinetic signal of a single cell. Top left, bright-field image. Bottom left, fluorescence image. Right, signal (I_B/I_D) as a function of time; each curve represents the signal of a single cell. Black line indicates the relocation within droplets with nonsecreting cells. **d**, Schematic representation of nanoparticle coating for IgG detection. The bioassay comprises paramagnetic nanobeads functionalized with anti-mouse kappa light chain V_HH, which captures IgG and binds it to the bead surface. **e**, Detection of murine recombinant IgG1 (circles) and IgG2 (squares) in 50-pL droplets. Top left, bright-field image. Bottom left, fluorescence image. Right, signal (I_B/I_D) as a function of IgG concentration (IgG1 detection reagent; red; IgG2 detection reagent, green). **f**, Time course analyses of IgG secretion of individual B cells. Top left, bright-field image. Bottom left, fluorescence image. Right, signal (I_B/I_D) as a function of time; each curve represents the mean signal of a single cell (IgG1, red; IgG2, green). Black line indicates the relocation within droplets with nonsecreting cells. Scale bars, 25 μm.

nanoparticles per droplet defines the capacity of the immunoassay and can be adjusted to the expected secretion rates to enable optimal results. However, a certain minimum value (100–200 beads/droplet) must be met to form a measurable beadline.

Secreted molecules are captured onto paramagnetic nanoparticles for detection, typically via capture antibodies. The immobilization of capture antibodies onto the nanoparticles is a critical step for the success of the protocol[55–60]. The performance of antibody-based biosensors is directly related to the orientation of antibodies on the nanoparticles and the accessibility of the paratope that binds the targeted analyte. In this protocol, we describe the use of two targeted coupling strategies. First, we describe a boronic acid (BA)-based coupling strategy for precise orientation of capture antibodies on

the surface of magnetic nanoparticles[55,61–63] (Fig. 3a–c). Second, we discuss a strategy based on biotinylated capture antibodies coupled to streptavidin-coated nanoparticles (Fig. 3d–f).

Automated image acquisition (Steps 38–45)

To perform imaging, the microfluidic chamber is placed on a motorized stage of an inverted epi-fluorescence microscope. In our case, 10× magnification was used as a compromise between scanning time and resolution for object detection within each droplet. We image between 75 and 225 fields of view in multiple channels (up to five, depending on the integrated assays): Using 75 fields of view (135 mm^2) results in ~60,000 imaged droplets, that is, 10,000–20,000 cells. Throughput can be improved by increasing the imaged area. However, when scanning large areas of a sample with high resolution, scanning time, as well as processing time (of large amount of imaging data), can become limitations of the throughput of the procedure. Here, binning of pixels during acquisition may help to solve some of these issues.

Because both automated object detection and fluorescence intensity measurements rely on focus quality, control of focus drift throughout the imaging procedure (of a large area over long times) is critical. Mechanical effects, vibrations, thermal changes and droplet movement can cause the focus to drift. We addressed this limitation by using the Perfect Focus System (PFS) of the Nikon microscope, but other microscopes may offer similar solutions.

Cell preparation, encapsulation and incubation within droplets (Step 46A/46B)

This analytical system is suitable for many different cells from various tissues and species. Primary cells are sensitive and fragile; therefore, requiring gentle handling during extraction and manipulation. Owing to the quantitative nature of the measurements described in this protocol, even small deviations might result in substantial differences. Gentle handling and rapid extraction of cells are important, and for optimal results, the cells should be present as a singularized suspension. Before encapsulation, the cell density must be adjusted so that the frequency of droplets containing a single cell is maximized and that of droplets containing multiple cells is minimized (see Box 3)[35].

Compartmentalization of cells within droplets will further affect cell survival. The surfactant is a key reagent for the droplet assays[35,64]; it must be non-cytotoxic, and it must stabilize droplet interfaces and prevent the coalescence of droplets during incubation. The use of a nonionic perfluoropolyether (PFPE) fluorosurfactant (600-g/mol PFPE tails and 2,000-g/mol heads)[35] in combination with fluorinated carrier oils such as HFE-7500 is recommended. At some point, nutrient depletion and pH changes will be a limiting factor for long-term studies of the encapsulated cells. The in-droplet pH is maintained by the addition of HEPES[65], and the fluorinated oil, which can dissolve ~20× more oxygen than water[66], used as a continuous phase, additionally serves as an, albeit limited, oxygen reservoir[67,68]. In addition, because fluorinated oils are very poor solvents for non-fluorinated molecules[69,70], they are well suited to cell-based and biochemical assays. Various biocompatible fluorinated oils and fluorosurfactants can be ordered from a large number of suppliers, such as 3M, RAN Biotechnologies, Dolomite, Sphere Fluidics and Bio-Rad. We confirmed the survival of primary monocytes over a 12-h time span, as well as the survival of primary murine splenocytes over the same time period, in 50-pL droplets. Furthermore, we added to our protocol a simple and sensitive cytotoxicity assay to discriminate dead from live cells to exclude any signals that might stem from dead or dying cells.

Image processing (Step 47A/47B)

We developed a robust, custom-made MATLAB-based program to detect and, if necessary, track droplets in time-lapse image sequences and to monitor the status of their content over time. The software analyzes the images over time in different fluorescence and bright-field channels. First, the droplets are detected in bright-field images using an algorithm that detects circles of a given diameter. In the next step, a binary mask of the detected droplets is generated, and this mask is overlaid onto the following fluorescence images to analyze each droplet separately. Within each droplet, the software measures the fluorescence of droplets, cells and beadlines (Fig. 4).

The software output is a spreadsheet containing morphological and fluorescence intensity parameters for different intra-droplet objects or regions over time. All measured fluorescence intensities on objects (i.e., magnetic beadline, cell or whole droplet) are normalized to the background fluorescence of the droplet to compensate locally for potential heterogeneity of illumination of the field, increase the sensitivity (signal-to-noise ratio differentiates better than the raw beadline signal), and reduce the impact of photobleaching on results.

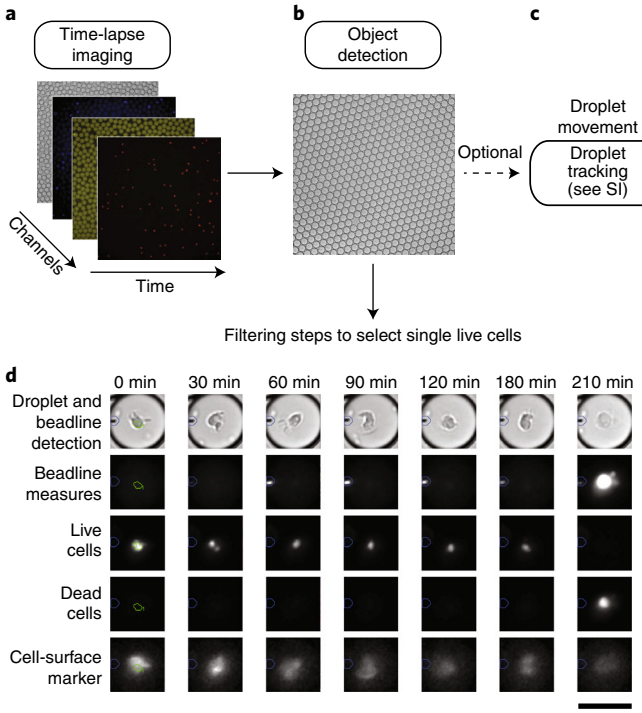

Fig. 4 | Analysis pipeline. a, Acquisition of images of the monolayer of droplets, illustrated for a single field of view in five imaging channels. Measurements were repeated at regular time intervals. **b**,**c**, Detection of droplet contours in the field (**b**) and of the intra-droplet beadline (bright-field image; **c**). Tracking of droplets allows continued analysis in spite of potential small droplet movements (Supplementary Fig. 3 and Supplementary Method 1). **d**, Images illustrating multiplexed and dynamic analyses of single monocytes. The droplet sub-image is shown in the five different imaging channels. Bright-field microscopy is used to detect droplets and magnetic beadlines; a Cy3 cube (orange fluorescence) is used to detect the secreted TNF-α on the beadline; a Cy5 cube (far-red fluorescence) is used to detect living cells; a GFP cube (green fluorescence) is used to detect dead cells; and a DAPI cube (blue–violet conjugate fluorescence) is used to detect cells expressing the cell-surface marker CD14. The $CD14^+$ monocytes remained alive over 180 min, and TNF-α relocalization on the beadline was detected 60 min after stimulation in droplets at 37 °C. At 180 min, the cells show an apoptotic activity, indicating the death of the cell. Live and dead monocytes were determined by staining with MitoView and NucView to measure mitochondrial membrane potential and caspase-3 activity, respectively. Scale bar, 50 μm. SI, supplementary information.

Materials

Biological materials

- Human blood. See Table 1 for characteristics of healthy donors and septic patients who participated in our study **! CAUTION** Experiments using human blood samples must conform to the relevant institutional and national regulations and require informed consent from all participants. For our experiments, samples from septic shock patients (Table 1) were obtained from the prospective cohort MICROFLU-SEPSIS, which was approved by the French Ethical Committee CPP Sud Ouest et Outre Mer 4 (registration no. 2017-A01134-49). Patients were admitted to the medical intensive care unit of Cochin Hospital, and informed consent was obtained from all participants or their legally authorized representatives. For the sepsis application, blood sample collection from healthy donors was performed according to the Ethical Committee of the Investigation Clinique et Acces aux Ressources Biologiques (ICAReB) platform (M.-N. Ungeheuer, Centre de Recherche Translationnelle, Institut Pasteur) as part of the DIAGMICOLL or CoSImmGEn (N° CORC: 2008-16 and 201-06) protocol, which was approved by the French Ethical Committee (CPP), Ile-de-France. Informed consent was obtained from all donors (Table 1). For the cytokine-secreting T-cell application, peripheral human blood was collected from healthy patients at the "Etablissement Français du Sang." Donors were recruited after a medical selection process complying with French regulations, and they gave their informed consent to participation in the study.
- Mouse spleen and bone marrow. In this protocol, we used *Mus musculus* BALB/cJRj females, age 8–10 weeks at the start of the immunization, supplied by Janvier Laboratories (cat. no. JAX #000651)

Table 1 | Characteristics of healthy donors and septic patients at admission to the intensive care unit

	Gender	Age	Sepsis source	SOFA[a]
Septic patient 1	Male	61	Cutaneous	8
Septic patient 2	Female	88	Urinary tract	6
Septic patient 3	Female	63	Osteo-articular	8
Healthy donor 1	Male	47	NA	NA
Healthy donor 2	Female	42	NA	NA
Healthy donor 3	Female	35	NA	NA

NA, not applicable. [a]The SOFA (Sequential Organ Failure Assessment) score is a bedside-applicable score designed to score organ dysfunction with less focus on mortality prediction.

! CAUTION Experiments using animal samples must conform to the relevant institutional and national regulations. In this work, the mouse experiments were validated by the CETEA Ethics Committee (no. 89; Institute Pasteur) under no. 2013-0103 and by the French Ministry of Research under agreement no. 00513.02 and were part of a larger scientific study.

Reagents

! CAUTION Wear appropriate protective clothing and equipment when manipulating chemical and biological reagents.

- Ultrapure DNase/RNase-free distilled water (Invitrogen, cat. no.10977049)
- Isopropanol (VWR, cat. no. 208224321) **! CAUTION** Isopropanol liquid and vapor are highly flammable. Handle away from ignition sources and flame.
- Acetone (VWR, cat. no. 322201) **! CAUTION** Acetone liquid and vapor are highly flammable. Handle away from ignition sources and flame.
- Ethanol (VWR, cat. no. 208224321) **! CAUTION** Ethanol liquid and vapor are highly flammable. Handle away from ignition sources and flame.
- 1H, 1H, 2H, 2H-Perfluorododecyltrichlorosilane (Sigma-Aldrich, cat. no. 729965) **! CAUTION** This reagent is corrosive and moisture sensitive. Work in a fume hood to avoid inhalation of silane.
- HFE-7500 oil (3M, cat. no. 98-0212-2928-5) **! CAUTION** Avoid direct contact with this liquid because it may cause respiratory, skin and eye irritation.
- Fluorinated surfactant (Ran Biotechnologies, cat. no. 008)
- SYLGARD 184 Silicone Elastomer Kit 1.1 KG Kit (Dow, cat. no. 1673921)

Application to sepsis

- Bovine serum albumin (BSA; Sigma-Aldrich, cat. no. A7960)
- Roswell Park Memorial Institute (RPMI) 1640 Medium GlutaMAX (Gibco, cat. no. 61870010)
- Phosphate-buffered saline (PBS; Dominique Dutscher, cat. no. L0612-500)
- Penicillin–streptomycin (Life Technologies, cat. no. 15140-122)
- HEPES (Dominique Dutscher, cat. no. L0180-100)
- Fetal bovine serum (FBS; HyClone cat. no. SH30070.03)
- Anti-CD14, blue violet conjugate (clone: TÜK4; Miltenyi Biotec, cat. no. 130-094-364, RRID: AB_10831023)
- Capture anti-TNF-α antibody (antibody TNF5; Mabtech, cat. no. 3510-6-1000, RRID: AB_907379; order a non-biotinylated form)
- Detection PE-anti-TNF-α antibody (clone: cA2; Miltenyi Biotec, cat. no. 130-120-489 without azide, cat. no. 120-014-229, RRID: AB_2752115)
- Recombinant TNF-α protein (BioLegend, cat. no. 570108)
- NucView488 (Biotium, cat. no. 99949)
- MitoView633 (Biotium, cat. no. 99950)
- LPS (lipopolysaccharide; Sigma-Aldrich, cat. nos. L2637, 3012 and 3137) **▲ CRITICAL** A mixture of three different LPS is prepared to ensure proper cell activation.
- Dextran (20% (wt/wt), 500 kDa; Sigma-Aldrich, cat. no. D8802)
- Carboxyl Adembeads (300-nm diameter; Ademtech, cat. no. 2131)

- EDC ((1-ethyl-3-(3-dimethylaminopropyl)carbodiimide hydrochloride); Thermo Fisher Scientific, cat. no. 77149) ▲ **CRITICAL** This material is moisture sensitive. Upon receipt, make aliquots and store them at −20 °C. This product is stable for 1 year.
- SulfoNHS (*N*-hydroxysulfosuccinimide; Thermo Fisher Scientific, cat. no. 24510) ▲ **CRITICAL** This material is moisture sensitive. Upon receipt, store at 4 °C. This product is stable for 1 year.
- Ethanolamine (Sigma-Aldrich, cat. no. E9508) ! **CAUTION** This material is an irritant. Work in a fume hood.
- Activation buffer (10×, for carboxyl-Adembead coupling; Ademtech, cat. no. 10101)
- Storage buffer (10×; Ademtech, cat. no. 10201)
- 3-Aminophenylboronic acid hemisulfate salt (Sigma, cat. no. A71751)
- EasySep Direct Human Monocyte Isolation Kit (STEMCELL Technology, cat. no. 19669)
- Ammonium chloride solution (StemCell Technologies, cat. no. 07800)

Application to murine IgG-secreting cells

- KnockOut Serum Replacement (Thermo Fisher Scientific, cat. no. 1082808)
- Human serum albumin, recombinant (rHSA); Sigma-Aldrich, cat. no. A9731)
- HEPES (Thermo Fisher Scientific, cat. no. 15630080)
- PBS (Thermo Fisher Scientific, cat. no. 14190250)
- Penicillin–streptomycin (Life Technologies, cat. no. 15140-122)
- Pluronic F-68 (10% (wt/vol) sterile filtered solution; Thermo Fisher Scientific, cat. no. 24040032)
- Pluronic F-127 (10% (wt/vol) sterile filtered solution; Thermo Fisher Scientific, cat. no. P6866)
- RPMI 1640 medium without phenol red (Thermo Fisher Scientific, cat. no. 11835030)
- Bio-Adembeads (streptavidin plus; 300-nm diameter; Ademtech, cat. no. 03132)
- CaptureSelect biotin anti-LC-kappa (murine) conjugate (Thermo Fisher Scientific, cat. no. 7103152100)
- AffiniPure F(ab')$_2$ fragment rabbit anti-mouse IgG, Fcγ fragment specific (Jackson ImmunoResearch Labs, cat. no. 315-606-047, RRID: AB_2340252)
- CellTrace Violet Cell Proliferation Kit (Thermo Fisher Scientific, cat. no. C34557)
- Zenon Alexa Fluor 488 Mouse IgG2b Labeling Kit (Thermo Fisher Scientific, cat. no. Z25202, RRID: AB_2736943)

Application to cytokine-secreting T-cells

- IFN gamma monoclonal antibody (MD-1; Thermo Fisher Scientific, cat. no. 14-7317-85, RRID: AB_468474), biotinylated in house
- IFN gamma monoclonal antibody (clone 4S.B3, APC conjugate; Thermo Fisher Scientific, cat. no. 17-7319-82, RRID: AB_469506)
- TNF-α monoclonal antibody (MAb1; Thermo Fisher Scientific, cat. no. 14-7348-85, RRID: AB_468488), biotinylated in house
- TNF-α monoclonal antibody (MAb11, PE (phycoerythrin) conjugate; Thermo Fisher Scientific, cat. no. 12-7349-81, RRID: AB_466207)
- IL-2 polyclonal antibody, biotin (Thermo Fisher Scientific, cat. no. 13-7028-81, RRID: AB_466900)
- IL-2 rabbit anti-human (PeproTech, cat. no. 500-P22-100ug, RRID: AB_147898), labeled in house with Alexa 555
- Alexa Fluor 555 NHS Ester (succinimidyl ester; Thermo Fisher Scientific, cat. no. A20009)
- Phorbol 12-myristate 13-acetate (PMA) (SigmaAldrich, cat. no. P1585)
- Ionomycin calcium salt (SigmaAldrich, cat. no. I3909)
- IL-4 monoclonal antibody (MP4-25D2), biotin conjugate (Thermo Fisher Scientific, cat. no. 13-7048-81, RRID: AB_466904)
- IL-4 monoclonal antibody (8D4-8), APC conjugate (Thermo Fisher Scientific, cat. no. 17-7049-81, RRID: AB_469497)
- Anti-human CD3, clone HIT3a, Alexa Fluor 647 conjugate (BioLegend, cat. no. 300322, RRID: AB_493693)

Equipment

General lab equipment

- Gloves (powder-free nitrile; Crolex)
- Microscope slides (frosted, ground edges; VWR, cat. no. 63115553)
- UV-curable glue (Norland Optical Adhesive, cat. no. 68 P/N 6801)
- FastRead 102 slides (Dominique Dutscher, cat. no. 390498)

- Reusable biopsy punches (diameters: 0.75 mm and 6 mm; WPI, cat. nos. 504529 and 504532)
- Sterican needles (23 gauge for 0.56-mm-diameter microtubing; Braun, cat. no; 921021)
- Sterican needles (27 gauge for 0.30-mm-diameter microtubing; Braun, cat. no. 921018)
- PTFE microtubing (0.56 × 1.07 mm; Fisher Scientific, cat. no. 1192-9445)
- PTFE microtubing (0.30 × 0.76 mm; Fisher Scientific, cat. no. 1191-9445)
- Sterile syringes (1 ml; Braun Omnifix, cat. no. 9204512)
- Sterile low-binding microcentrifuge tubes (Dominique Dutscher, cat.no 27210)
- Petri dishes (100-mm diameter × 15 mm; BD Falcon, cat. no. 351029)
- Nanoport 6-32 (Cil, cat. no. N-126-01)
- Cap (Cil, cat. no. P-555)
- MicroTight fittings (Cil, cat. no. P126S)
- Three low-pressure syringe pumps (Cetoni, model no. neMESYS 290N) and control module (Cetoni, model no. Base 120)
- Vortex (LMS; Dominique Dutscher, cat. no. 079030)
- Adjustable pipettes (2.5-, 10-, 20-, 200- and 1,000-µl; Eppendorf, cat. nos. 3123000012, 3123000020, 3123000039, 3123000055 and 3123000063)
- Sterile pipette tips (10-, 20-, 200- and 1,000-µl, ART; Thermo Fisher Scientific, cat. nos. 2140-HR, 2149P-HR, 2069-HR and 2179-HR)
- Carousel holder for six micropipettes Research or six multipettes (Dominique Dutscher, cat. no. 33076)
- Smart Spatula (Dominique Dutscher, cat.no. 059362)
- Centrifuge (Eppendorf, model no. 5810R and 5418R)
- Magnet holder for 1.5 microtube (Ademtech, cat. no. 20101)
- EasySep magnet (StemCell Technologies, cat.no. 180001) **! CAUTION** The magnet has a strong magnetic field. Handle it carefully and keep it away from objects that respond to magnetic fields.
- Round-bottom polystyrene Falcon tubes (5 and 15 ml; Dominique Dutscher, cat. nos. 352235 and 352051)
- Rapid-flow filter unit (0.2-µm PES membrane. 0.75 mm; Thermo Fisher Scientific, cat. no. 566-0020)
- Sonicator (Bransonic, model no. B200 ultrasonic cleaner; Dominique Dutscher, cat. no. 910586)
- Mini shaker vortex (Lab Dancer; Dominique Dutscher, cat. no. 250097)
- Rotating shaker (Stuart SB3; Dominique Dutscher, cat. no. 250097)
- Drum 40 microtubes (1.5 ml; Dominique Dutscher, cat. no. 90435)
- Inverted microscope for droplet generation (Olympus, model no. IX83)
- Microtiter microplate (96-well; Greiner, cat.no. 650185)
- Dark microtiter plate (96-well; Corning, cat.no. 3991)
- Magnet holder for 96-well plate (Ademtech, cat. no. 20106)
- Plate reader (Tecan, model no. infinite M200 Pro)
- Scotch tape (3M, cat. no.7100024666)
- Filter (0.22-µm; Millipore)

Chip fabrication

- Disposable mixing cups (Dominique Dutscher, cat. no. 045108)
- Aluminum foil (Alupro, cat. no. A0626)
- Oven (Binder 300 °C, Dominique Dutscher cat. no. 9010-0190)
- Vacuum desiccator (Sigma-Aldrich, cat. no. D2672)
- Scalpel (no. 11; Becton Dickinson, cat. no. 371611)
- Oxygen plasma cleaner (Femto Science, CUTE.MRP model)

Chamber fabrication

- UV light source 5 (Opticure LED; Tech Optics LED, cat. no. 5090-200)
- Tweezers (dark blue forceps, 111 mm; Dutscher, cat. no. 037876)
- CO_2 laser (AxysLaser, model no. C180 ii-CO2) or alternative tool for drilling 1-mm holes in glass
- Cutting plotter (Graphtec, model no. CE6000-40) or Cameo plotter (Silhouette)

Chamber fabrication for sepsis application

- Double-sided adhesive tape (Adhesive Research, cat. no. 92712)
- Binder clips (SafeTool, cat. no. 8140.19 or 8140.32)
- Magnet (First4Magnets, cat. no. F75103) **! CAUTION** These magnets are powerful. They can be dangerous; handle them carefully. Keep them away from objects that respond to magnetic fields.
- Oven (Binder 300 °C; Dominique Dutscher cat. no. 9010-0190)

Chamber fabrication for IgG application

- Orafol Tape Series 1375 (SDAG Adhésifs)
- Silicone paper (135 g/m^2; SDAG Adhésifs) ▲ **CRITICAL** The Orafol 1375 tape is covered with paper on only one side. Use this tape to cover the other side, and cut through this tape in the assembly to generate optimal results for chamber fabrication.
- Magnets (two; K&J Magnetics, cat. no. BZX082) ! **CAUTION** These magnets are powerful. They can be dangerous; handle them carefully. Keep them away from objects that respond to magnetic fields.
- 3D-printed holder for magnets (build according to Supplementary Data 4)
- Thermal press capable of a pressing 7 bar and heating to 150 °C (Scamex)

Microscope and image acquisition

- Inverted microscope for time-lapse imaging (Nikon, model no. Eclipse Ti-2E)
- Digital CMOS camera; 2,048 × 2,048 with pixel array with 6.5 × 6.5-μm^2 pixel size (Hamamatsu, model no. ORCA Flash 4 LT)
- Transmission light source (powerful white LED; CoolLED, cat. no. pE-100wht). It replaces the typical 100-W halogen lamp.
- LED-based excitation light engine (Lumencor, cat. no. SOLA SE II,). It replaces mercury arc lamp.
- Objective (10× CFI Plan Apochromat; Nikon, cat. no. MDR00105)
- Microscope enclosure and temperature controller (Okolab, cat. no. H201-T-UNIT-BL)
- Motorized *xy* stage (Nikon, cat. no. MECS MEC56110)
- Software for stage control and image acquisition (Nikon, cat. no. NIS-AR Log MQS3 1000)
- Perfect Focusing System 2 (PFS2; Nikon, cat. no. MEP59390) ▲ **CRITICAL** The PFS2 system is needed to retain focus over large measurement areas.
- DAPI fluorescence cube (excitation (ex.) 377/50 nm, emission (em.) 447/60 nm, cutoff 409 nm; Nikon, cat. no. DAPI-5060C)
- GFP fluorescence cube (ex. 482/18 nm, em. 520/28 nm, cutoff 495 nm; Nikon, cat. no. GFP-1828A)
- CY3 fluorescence cube (ex. 531/40 nm, em. 593/40 nm, cutoff 562 nm; Nikon, cat. no. CY3-4040C)
- CY5 fluorescence cube (ex. 628/40 nm, em. 692/40 nm, cutoff 660 nm; Nikon, cat. no. CY5-4040C)

Software and analysis workstation

- MATLAB (MathWorks, v. 2018a or later, licensed, https://fr.mathworks.com/downloads/)
- MATLAB Image Processing Toolbox (MathWorks, licensed, https://www.mathworks.com/products/image.html)
- VLFeat open-source library (https://www.vlfeat.org/install-matlab.html)
- MATLAB image analysis workstation: eight virtual processors, 2.6 GHz, 64 GB RAM
- DropCell.exe (https://figshare.com/articles/DropCell_exe_installer/11336663/1) ▲ **CRITICAL** Before first use of the MATLAB application, it will have to be installed on your computer. This is done automatically by running the provided MyAppInstaller_web.exe file (provided by BIOASTER, https://figshare.com/articles/DropCell_exe_installer/11336663/1). The same installer file will offer to download and install the required v. 9.4 (R2018a) of the MATLAB Runtime, if not already installed on your machine. An example of the input_parameters.txt file, as well as a readme_dropcell.txt file, will be automatically copied to the folder where you will choose to install the application ▲ **CRITICAL** Read the readme_dropcell.txt carefully before your first use of DropCell.exe. It describes the installation procedure as well as the naming rules for the input images.

Reagent setup

Silane solution

To prepare 1% (vol/vol) silane solution, dilute 10 μl 1H, 1H, 2H, 2H-perfluorododecyltrichlorosilane in 990 μl filtered HFE-7500 oil. This solution should be prepared immediately before use ! **CAUTION** This solution is an irritant and corrosive; work in a fume hood with appropriate materials ▲ **CRITICAL** Use this reagent immediately after preparation.

Coupling buffer (for boronic-based functionalization)

Dilute activation buffer 10-fold in pure distilled water. This buffer should be freshly prepared before use.

Storage buffer for boronic-based functionalization

Dilute storage buffer 10-fold in pure distilled water. This buffer should be freshly prepared before use.

Quenching buffer for boronic-based functionalization
Quenching buffer is 100 mM ethanolamine in PBS. This buffer should be freshly prepared before use. **! CAUTION** This solution is corrosive and irritating; work in a fume hood. **▲ CRITICAL** Use this reagent immediately after preparation. Do not store.

Blocking buffer for boronic-based functionalization
Blocking buffer is 1% (vol/vol) dextran. Dilute 20% (wt/wt) dextran 20-fold in pure distilled water to obtain 1% (vol/vol) blocking buffer. This solution can be stored at 4 °C for up to 6 months. **! CAUTION** The 20% (wt/wt) dextran is viscous; pipette this solution very slowly.

Cell buffer 1 for sepsis application
Heat the FBS at 56 °C in a water bath for 35 min. Cool to room temperature (20–25 °C) and filter the serum with a rapid-flow filter unit (0.2 µm-PES membrane). Make 50-ml aliquots and store at −20 °C. After thawing an aliquot, centrifuge the serum at 3,000*g* for 10 min at room temperature to remove large debris. Supplement RPMI 1640 Medium GlutaMAX with 10% (vol/vol) heat-inactivated FBS, 5% (vol/vol) penicillin–streptomycin and 20 mM HEPES. Store cell buffer at 4 °C and use it within 2 weeks after preparation.

Blocking buffer for murine IgG application
Blocking buffer is 5% (vol/vol) Pluronic F-68 in PBS, sterile. The buffer can be stored at −20 °C in small aliquots until ready to use. For short-term storage, store at 4 °C for up to 4 weeks.

Cell buffer 2 for IgG application
Cell buffer 2 is RPMI 1640 (without phenol red) supplemented with 10% (vol/vol) KnockOut Serum Replacement, 1× penicillin–streptomycin, 0.1% (vol/vol) Pluronic F-127, 0.5% (wt/vol) rHSA and 25 mM HEPES. Make aliquots of cell buffer 1 and freeze at −20 °C. For short-term storage, store at 4 °C for up to 1 week. The buffer can be stored for up to 4 weeks if working in a sterile environment **▲ CRITICAL** The use of rHSA and the removal of all products of animal origin reduces assay background and increases sensitivity.

Immobilization reagent for IgG application
This solution is CaptureSelect biotin anti-LC-kappa (murine) conjugate (stock concentration: 1 mg/ml) diluted 1:5 (vol/vol) in PBS. Make 50-µl aliquots and store at −20 °C. For short-term storage, store at 4 °C for up to 4 weeks.

Procedure

Microfluidic device fabrication from existing molds ● Timing 4 h

▲ CRITICAL Follow the instructions by Mazutis and colleagues[35] to design microfluidic chips and fabricate the wafer mold (see Supplementary Data 1 for our wafer design). Ready-to-use wafer molds can be obtained from various commercially suppliers, thus avoiding photo-lithography steps (not described here; see reference[71]). Furthermore, finished droplet makers can be obtained directly from a variety of commercial suppliers, such as Dolomite, Elveflow and others, to avoid Steps 1–22. If purchased, droplet makers should be capable of forming 50-pL droplets.

1 Place the wafer mold on a circular piece of aluminum foil (~2-cm-larger diameter than wafer). Form a cup around the mold.
2 Dust off the wafer mold with compressed nitrogen or air.
▲ CRITICAL STEP Care should be taken to remove any dust that might form clumps in the channels.
3 Place the aluminum foil cup containing the mold into a Petri dish.
4 Per wafer, pour 45 g of PDMS and 5 g of curing agent (9:1 (wt/wt) PDMS/curing agent ratio) into a disposable beaker and vigorously mix with a 1,000-µl pipette tip or a plastic fork.
▲ CRITICAL STEP Do not forget to add the curing agent; mix thoroughly. It is difficult to remove non- or semi-cured PDMS from the wafer mold.
5 Degas the PDMS–curing agent mixture with a vacuum chamber until all air bubbles are removed.
6 Slowly poor the degassed PDMS–curing agent mixture on top of the wafer mold from Step 3.
7 Put the Petri dish under vacuum again and degas the PDMS until no bubbles are visible. If bubbles persist, gently remove remaining bubbles with an air blower and then cover the Petri dish with a lid to protect the PDMS from dust.

8 Bake the Petri dish containing the wafer mold in a drying oven at 65 °C for 90–120 min to harden the mixture.

9 Cool the Petri dish to room temperature and carefully peel off the PDMS from the wafer mold with a scalpel. Clean the PDMS and wafer with clean nitrogen or air.
▲ **CRITICAL STEP** The wafer is very fragile; any excessive pressure or bending force will break it. Wear protective glasses. Remove any PDMS from the wafer's bottom side first, and slowly remove the PDMS from the wafer by carefully lifting the PDMS from the edges. The wafer can be reused many times when handled properly.
■ **PAUSE POINT** The cured PDMS can be stored in a dust-free environment (Petri dish) at room temperature for several months.

10 Place the PDMS on a cutting mat with the patterned side facing upward. Cut the PDMS into separate microfluidic chips with a scalpel.

11 Use a biopsy punch (diameter: 0.75 mm) to punch holes into the indicated places (inlet and outlet holes, four per chip; see Supplementary Data 2 for the mask for the double-sided tape to prepare the observation chamber) to allow the outside connections.
▲ **CRITICAL STEP** The diameter of the biopsy punch is critical. We use a 0.75-mm-diameter biopsy punch to make inlet holes into which a 200 µl pipette tip fits tightly (for aqueous phases; Supplementary Fig. 1) and 0.3-mm PTFE microtubing (for the oil phase).
? TROUBLESHOOTING

12 Cover both sides of the PDMS slab with frosted Scotch tape and then peel off the tape from both sides to remove PDMS debris that may be formed during punching. Alternatively, dust off the PDMS slabs with compressed air or nitrogen to remove any remaining PDMS debris.
▲ **CRITICAL STEP** Repeat Step 12 if necessary. Care should be taken to remove any resulting PDMS debris or dust that could otherwise clog the microfluidic chip.

13 Place a clean glass slide and the PDMS slab in the plasma chamber with the patterned side facing upward.

14 Run the oxygen plasma program, following the manufacturer's recommendations. We use 30 s and 35 W.
? TROUBLESHOOTING

15 Carefully remove the glass slide and PDMS slab from the plasma chamber; then bring the treated surfaces into contact. Press the PDMS slab gently onto the glass slide to ensure uniform bonding.
▲ **CRITICAL STEP** To avoid microfluidic channel collapse and damage, press only gently on the PDMS slab. If plasma activation is successful, the chip will attach almost by itself.
▲ **CRITICAL STEP** Contact between PDMS slab and glass slide should be made quickly after plasma exposition to avoid the hydrophobic reconstitution of PDMS (<5min). Be careful when placing the PDMS; once contact is established, PDMS parts cannot be moved or removed.
? TROUBLESHOOTING

16 Place the microfluidic device in the oven at 90 °C for 5–20 min.
▲ **CRITICAL STEP** The chip needs surface treatment for the formation of droplets. Perform this step directly after plasma treatment and bonding.

17 Remove the device from the oven and cool it at room temperature.

18 Connect a 27-gauge needle to a piece of 0.30-mm-diameter PTFE microtubing using tweezers. Fill a 1-ml syringe with silane solution; afterward attach a 0.22-µm filter to the syringe. Connect the needle microtubing to the syringe filter and fill the whole assembly with silane solution. Prepare a second syringe filled with filtered HFE-7500 only.
! **CAUTION** Use tweezers to hold the tubing. Take care to not pierce your skin.
! **CAUTION** 1H, 1H, 2H, 2H-Perfluorododecyltrichlorosilane is corrosive and highly irritant upon inhalation. Work in a fume hood. Store the product under argon; or make aliquots and freeze because the silane will react rapidly with humid air and form crystals.

19 Put the microtubing into the oil inlet and flush the microfluidic channels with silane solution for about 10–30 s.

20 After 1-min incubation, flush the device with compressed clean air or nitrogen.
! **CAUTION** Stay clear of the aerosols; work under fume hood. We attach a 200-µl pipette tip to the gas outlet to facilitate the connection.

21 Repeat Steps 19 and 21 twice with pure HFE-7500 oil to wash the microfluidic device.

22 Use a light microscope to check for dust inclusion in the microfluidic device, especially at the orifice for droplet generation. If dust is present, mark the chips and do not use them. Cover the PDMS chip with Scotch tape.

■ **PAUSE POINT** The microfluidic chip can be stored in a closed box at room temperature for several months. Care should be taken to protect the devices from dust.

? TROUBLESHOOTING

Production of chamber mask in double-sided tape for the observation chamber ● Timing 10 min

23 Load the provided mask for the double-sided tape (see Supplementary Data 2 for the mask for the double-sided tape to prepare the observation chamber) into the cutting plotter.

24 Load the double-sided tape into the plotter and initiate the machine according to the user handbook.

25 Use the relevant plotter software (Graphtec or Silhouette Cameo) to send the design to the plotter. Use the following conditions for plotting with the Graphtec Cutting plotter:

Parameter	Setting
Offset	0
Speed	25
Acceleration	1
Cut force	21
Blade offset	2.1

Or use these conditions with Silhouette Cameo:

Parameter	Setting
Blade setting	3
Speed	5 cm/s
Thickness	33

Plot the chamber design onto the double-sided tape; then cut it into rectangles with scissors.

▲ **CRITICAL STEP** The above settings will result in a plot that cuts the top protective layer and the double-sided tape but not the bottom protective layer.

■ **PAUSE POINT** The cut tape can be stored in a closed box at room temperature for several months.

Production of glass slides with access holes ● Timing 5 min per slide

26 Use laser ablation to produce two holes (diameter ~1 mm; see Supplementary Data 3 for the mask for laser ablation) in a 76 × 26 × 1-mm microscopy slide. The parameters for laser ablation will depend on the type of the machine used. We use the AxysLaser with 95% energy, 20 repetitions, and a 10-mm cluster to speed up the process.

▲ **CRITICAL STEP** If laser ablation is not available, good alternatives are drilling or sand-blasting. Take care to wear appropriate safety equipment when working with the glass.

27 Rinse and clean the glass slides with acetone. Repeat this process with isopropanol and then with clean water. Dry with compressed air or nitrogen. Also clean a glass slide without holes (for the bottom of the chamber).

■ **PAUSE POINT** The glass slides can be stored in a closed box at room temperature for several months.

Microfluidic chamber assembly

28 We use two variations of the same procedure to fabricate the droplet observation chamber. When using low numbers of beads (<500 beads per droplet, such as for the sepsis application) follow option A; when using high numbers of beads (>500 beads per droplet, such as for the murine IgG application) follow option B. Both are based on the use of double-sided tape and glass slides.

The principal difference between the procedures is the equipment needed to press the chamber (binder clips in option A; thermal press in option B).

(A) **Sepsis application** ● **Timing 3–5 h**

(i) Take a nanoport and place it on one of the outlet holes of the top microcopy slide (from Step 27). Use a 23-gauge needle to align the nanoport with the access holes on the glass slide (Fig. 2c).

(ii) Add a drop of a UV-curable glue at the base of the nanoport and cure with UV light.

! CAUTION Wear appropriate eye and skin protection when using UV light to cure the glue.

▲ CRITICAL STEP This step must be performed carefully to avoid clogging of the holes. Deposit a drop of viscous glue carefully; it should be introduced between the slide and nanoport by capillary forces (Fig. 2c). Make sure not to move the nanoport during this process.

(iii) Repeat Step 28A(i, ii) for the second hole, and then expose the glass to oxygen plasma.

(iv) Cover the top slide with the patterned double-sided adhesive tape (Fig. 2c, from Step 25) and then bring the bottom slide (from Step 27) into contact to form a 2D incubation chamber. Gently press the two slides together to ensure uniform sealing.

(v) Clamp the slides together with binder clips to seal the chamber (Fig. 2c)

(vi) Incubate the clamped device for at least 2 h at 90 °C.

(vii) Cool the chamber to room temperature and remove the clamps.

▲ CRITICAL STEP Inspect the sealing quality with an optical microscope; a well-sealed device should not contain Saffman-Taylor fingers (Fig. 2d).

? TROUBLESHOOTING

(viii) Attach a magnet to the bottom slide of the microfluidic chamber with double-sided adhesive tape (Fig. 2e). Proceed to Step 29.

! CAUTION This magnet is powerful and generates a strong magnetic field (0.22 T). Care should be taken during handling to keep the magnet away from objects that respond to magnetic fields.

▲ CRITICAL STEP The magnet is 3 mm thick, which is convenient for image acquisition with the inverted microscope. Do not heat the magnet because heating may affect the magnetization.

■ PAUSE POINT The chamber can be stored at room temperature for several months.

(B) **Murine IgG application** ● **Timing 1.5 h**

(i) Clean the two glass slides (top slide from Steps 26 and 27 and bottom microscopy slide from Step 27) in air plasma for 10 min. If plasma is not available, this cleaning step can be replaced with cleaning by frosted scotch tape or compressed air or nitrogen.

(ii) Remove the protective layer from the shaped double-sided tape and put the top slide (with holes) onto the adhesive tape. Flip it and carefully remove the second layer and bring the bottom slide into contact to form a 2D incubation chamber. Gently press the glass slides together to ensure uniform sealing.

▲ CRITICAL STEP Make sure to work in a clean and dust-free environment. In our experience, the tape tends to slightly adhere to the protective layers. To reduce this problem, the tape can be put at −20 °C before application. Remove it carefully to avoid rupture or form deposits of tape. Deposits of tape will result in a chamber of incorrect height, and the user will observe droplet movement during measurements.

(iii) Transfer the assembly to the thermal press; start and heat the thermal press to 150 °C.

(iv) Place the assembly at 150 °C for 5 min and press with 7 bars to achieve a chamber with a height of 33 ± 2 μm.

! CAUTION Use appropriate safety equipment. The glass will be hot and might crack under pressure if deposits of dust, tape or other impurities are present.

(v) Perform Step 28A(i, ii) to attach the two nanoports to the assembly.

(vi) Attach magnets on either the side of the chamber with UV glue, or directly at the microscope using an appropriate support (see Supplementary Data 4 for the mask for the magnet holder).

! CAUTION This magnet is powerful and generates a strong magnetic field. Care should be taken during handling; keep the magnet away from objects that respond to magnetic fields. If beadlines appear to be points, the magnetic field is vertical instead of horizontal.

■ PAUSE POINT The chamber can be stored at room temperature for several months.

Surface treatment of the chamber ● Timing 10 min

29 Repeat Step 18 and then connect the tubing to the nanoport with a MicroTight fitting adaptor.

30 Flush the chamber with 0.5–1 ml silane solution, incubate for 1–3 min, completely flush with nitrogen and then fill with 1 ml HFE-7500 oil. Close the assembly with two caps (Fig. 2e).
! CAUTION 1H, 1H, 2H, 2H-Perfluorododecyltrichlorosilane is corrosive and highly irritant upon inhalation. Work in a fume hood.
■ PAUSE POINT The chamber can be stored at room temperature for several months.

Nanoparticle functionalization

31 Use one of the two following approaches to functionalize the nanoparticles. One approach uses boronic acid coupling via glycosyl groups on the antibody to immobilize the antibody on the nanoparticles to measure TNF-α secretion by single monocytes (option A). The second approach uses the interaction between biotin and streptavidin to functionalize the beads to measure antibody secretion rate from and affinity of single B cells (option B).

(A) **Boronic acid coupling for sepsis application ● Timing 20 h (4 h hands-on)**

(i) Resuspend the carboxyl Adembeads by pipetting and vortexing.
▲ CRITICAL STEP Care should be taken to avoid foaming and bubble formation.
? TROUBLESHOOTING

(ii) Transfer 1 mg (33.33 µl) of beads to a clean 1.5-ml microtube.
! CAUTION Use a low-binding 1.5-ml tube to perform bead functionalization.

(iii) Add 100 µl of coupling buffer and vortex gently.

(iv) Place the tube in a magnet holder for about 1 min at room temperature to pellet the beads.

(v) Carefully discard the supernatant with a 200 µl pipette.
▲ CRITICAL STEP Do not disturb the bead pellet. A clear supernatant indicates a complete bead collection.

(vi) Remove the tube from the magnet holder and then vigorously resuspend the beads in 100 µl coupling buffer by vortexing.
▲ CRITICAL STEP Care should be taken during washing steps. Do not allow the beads to dry out. Drying reduces performance. After removing the supernatant, add buffer quickly.

(vii) Repeat Step 31A(iv–vi) twice to complete the washing.

(viii) Sonicate the beads for 3 min at room temperature at 30 W and 46 kHz. The beads are now ready for EDC–sulfoNHS-based activation.
! CAUTION Wear ear protection when sonicating beads.
▲ CRITICAL STEP Sonication breaks nanoparticle aggregates. The presence of aggregates reduces the efficiency of antibody coupling.

(ix) Put aliquots of EDC and sulfoNHS at room temperature for 5–10 min and prepare a 10 mg/ml solution for each.

(x) Mix 0.5 ml of EDC solution with 0.5 ml of sulfoNHS solution to form a 5 mg/ml solution of activated EDC–sulfoNHS.

(xi) Place the tube containing the beads in a magnet holder for about 1 min; then carefully discard the supernatant.

(xii) Resuspend the beads in 1 ml of activated EDC–sulfoNHS solution. Sonicate the beads for 3 min at room temperature.

(xiii) Incubate for 20 min on a rotating wheel at room temperature.

(xiv) Place the tube in a magnet holder for 1 min to pellet the beads.

(xv) Carefully discard the supernatant.

(xvi) Add 100 µl of coupling buffer to the beads (see 'Reagent setup').

(xvii) Remove the tube from the magnet holder and mix well by vortexing.

(xviii) Repeat Step 31A(xiv–xvii) twice. The beads are now activated and ready to react with boronic acid.

(xix) Weigh 50 mg of 3-aminophenylboronic acid hemisulfate salt and dissolve it in 1 ml coupling buffer.

(xx) Place the tube in a magnet holder for 1 min to pellet the beads.

(xxi) Carefully discard the supernatant.

(xxii) Resuspend the beads in 1 ml coupling buffer, and then sonicate them for 3 min at room temperature.

(xxiii) Incubate for 2 h on a rotating wheel at room temperature.

(xxiv) Place the tube in a magnet holder for about 3 min at room temperature.
(xxv) Carefully discard the supernatant. Do not disturb the bead pellet.
(xxvi) Add 100 µl of PBS to beads.
(xxvii) Remove the tube from the magnet holder and mix well by vortexing.
(xxviii) Repeat Step 31A(xxiv–xxvii) twice.
(xxix) Pellet the beads by placing the microtube in a magnet holder for 1 min.
(xxx) Carefully discard the supernatant. Do not disturb the bead pellet.
(xxxi) Resuspend the beads in 500 µl of 100 mM ethanolamine to quench the reaction.
! CAUTION Ethanolamine is an irritant; handle it carefully under a chemical hood.
(xxxii) Sonicate for 3 min and then incubate for 30 min at room temperature on a rotating wheel.
(xxxiii) Place the tube in a magnet holder for about 1 min at room temperature.
(xxxiv) Carefully discard the supernatant. Do not disturb the bead pellet.
(xxxv) Add 100 µl of PBS to the beads.
(xxxvi) Remove the tube from the magnet holder and mix well by vortexing.
(xxxvii) Repeat Step 31A(xxxiii & xxxvi) twice.
(xxxviii) Resuspend the beads in 50 µl PBS by vortexing and then sonicate for 3 min at room temperature.
(xxxix) Add 50 µg of antibody (50 µl of 1mg/ml solution) to 1 mg of boronic-coated beads.
! CAUTION The anti-TNF-α antibody is provided in PBS buffer without sodium azide. Users should work under a biological safety cabinet and aseptic conditions to avoid any contamination.
▲ CRITICAL STEP For optimal coupling we recommend testing 10–50 µg of antibody per milligram of boronic-coated beads. If other antibodies are used, the optimal value might be different.
▲ CRITICAL STEP Antibody coupling will be successful only if the antibody is glycosylated.
▲ CRITICAL STEP If other antibodies are used, the antibody solutions must be free of sodium azide, storage proteins or amine-based buffers (e.g., HEPES, MOPS, TRIS) that could interfere with the coupling procedure. If present, the buffer needs to be exchanged using a desalting spin column or similar.
(xl) Mix gently; then incubate overnight at 4 °C with gentle shaking.
(xli) After overnight incubation, place the tube in a magnet holder for 1 min to pellet the beads.
(xlii) Carefully discard the supernatant without disturbing the bead pellet.
(xliii) Add 100 µl of PBS to the beads.
(xliv) Remove the tube from the magnet holder and mix well by vortexing.
(xlv) Repeat Step 31A(xli–xliv) twice.
(xlvi) After washing, resuspend the beads in 200 µl storage buffer. The concentration of the beads should be 5 mg/ml (1 mg in 0.2 ml).
(xlvii) Sonicate the beads for 1–2 min at room temperature and store the antibody-coated beads at 4 °C.
▲ CRITICAL STEP Keep the beads at 4 °C and do not freeze. Freezing will cause the beads to aggregate and reduces the sensitivity of the bioassay.
■ PAUSE POINT The antibody-coated nanoparticles are stable for at least 2 months at 4 °C without affecting the performance of the bioassay. Longer storage times will need to be tested by users.
(xlviii) For experiments, vortex the beads vigorously for 1 min to resuspend the formed pellet.
(xlix) Resuspend 10 µL of antibody-coated beads in 100 µl blocking buffer.
▲ CRITICAL STEP Before using the beads in a binding assay, treat the beads with blocking buffer for boronic-based functionalization to reduce non-specific binding.
(l) Incubate for 45 min at room temperature with shaking at 700 r.p.m.
(li) Place the tube in a magnet holder for about 1 min to pellet the beads.
(lii) Carefully discard the supernatant. Do not disturb the bead pellet.
(liii) Add 100 µl of PBS buffer to the beads.
(liv) Remove the tube from the magnet holder and mix well by vortexing.
(lv) Repeat Step 31A(li–liv) twice.
(lvi) After the washing step, sonicate the beads for 1 min at room temperature. Use immediately for the assay.

(B) **Biotin–streptavidin coupling for the murine IgG application** ● **Timing 2 h**
(i) Resuspend the Bio-Adembeads (streptavidin plus) by vortexing for 10 s.
? TROUBLESHOOTING

Box 4 | Detection of protein of interest using a microtiter plate (bulk) assay ● Timing 3 h

▲ **CRITICAL** As an alternative to the droplet-based quality control assays of the functionalized nanoparticles, one can also perform a fluorescence-based sandwich immunoassay in microtiter plates. It should be noted that bulk assays use more reagents, and a calibration curve can also be performed directly within droplets to enable the quantitative measurement of secretion rates (Box 2, Fig. 3b,e).

Procedure

1 Prepare a serial dilution of the recombinant protein of interest (typically in the range 0–100 nM) in PBS containing 1% (wt/vol) BSA in a 96-well microtiter microplate. Final volumes should be 90 µl each.
2 Add 10 µl of functionalized nanoparticles to each well containing the protein of interest and then mix well by pipetting.
3 Incubate, with shaking at 700 r.p.m., for 1 h at room temperature.
4 Place the microtiter plate on a magnet holder for about 1 min at room temperature.
5 Carefully discard the supernatant. Do not disturb the bead pellet.
6 Add 100 µl of PBS buffer to beads.
7 Remove the microtiter plate from the magnet holder and mix well by shaking at 700 r.p.m. for 1 min.
8 Repeat steps 4–7 once.
9 Collect the beads, carefully discard the supernatant and then add 100 µl of solution containing 0.8 µg/ml fluorescence-labeled detection antibody to each well.
10 Incubate, with shaking at 700 r.p.m., for 1 h at room temperature.
11 Place the microtiter plate on a magnet holder for about 1 min at room temperature.
12 Carefully discard the supernatant. Do not disturb the bead pellet.
13 Add 100 µl of PBS buffer to beads.
14 Remove the microtiter plate from the magnet holder and mix well by shaking at 700 r.p.m. for 1 min.
15 Repeat steps 11–14 once.
16 Pellet the beads using the magnet and carefully discard the supernatant. Resuspend the beads directly in 50 µl PBS and mix gently by pipetting.
17 Transfer the samples to a black 96-well microtiter microplate and measure fluorescence at the wavelength optimal for the fluorophore on the detection antibody using the microplate reader.
18 Plot the curve of fluorescence intensity against the concentration of the added protein of interest.
? TROUBLESHOOTING

(ii) Per experiment, transfer 25 µl of beads to a clean low-binding 1.5-ml microtube. Add 25 µl of PBS per 25 µl of nanoparticles.
▲ **CRITICAL STEP** Adapt accordingly if more or less nanoparticles are wanted in a droplet (see also Boxes 1 and 2).

(iii) Add 2.5 µl of IgG immobilization reagent stock to each 50-µl bead solution. Deposit the drop at the top of the Eppendorf tube and wash it down with the beads. Mix by pipetting and incubate for 20–30 min at room temperature.
▲ **CRITICAL STEP** For other biotinylated antibodies, add 5 µl of a 0.5 mg/ml stock to a 100-µl nanoparticle volume. This concentration may need to be optimized.

(iv) Pellet the beads by placing the microtube in a magnet holder for about 1 min.

(v) Carefully discard the supernatant.
▲ **CRITICAL STEP** Do not disturb the bead pellet. A clear supernatant indicates a complete bead collection.

(vi) Remove the tube from the magnet holder and then vigorously resuspend the beads in 50 µl blocking buffer. Incubate for 20–30 min.
▲ **CRITICAL STEP** Care should be taken during washing steps to not lose particles because of inefficient resuspension or collection. Do not allow the beads to dry out because drying reduces performance.

(vii) Afterward, repeat Step 31B(iv and v).

(viii) Add cell buffer 2 (the same volume as used in Step 31B(ii)). Resuspend the beads and incubate for 20–30 min to block the bead surfaces.
■ **PAUSE POINT** The beads can be stored overnight at 4 °C after this step and used the next day.

(ix) Shortly before the experiments, repeat Step 31B(iv, v).

Quality control of functionalized nanoparticles

32 Assess the binding capacity of the immobilized antibody using a fluorescence-based sandwich immunoassay in microtiter plates (bulk assay; Box 4) or within droplets. For the droplet microfluidic assay for the sepsis application, follow option A. For the droplet microfluidic assay for the murine IgG application, follow option B.

(A) **Detection of TNF-α using a droplet microfluidic assay** ● Timing **2 h**

▲ CRITICAL Following this protocol and the respective dilutions will lead to a beadline capacity of ~3 nM within each droplet and a number of nanoparticles of ~170 per droplet.

(i) Prepare the syringes for the protein solutions by connecting 0.56-mm-diameter PTFE microtubing to 200-µl pipette tips using PDMS slabs (6-mm diameter, with a 0.75-mm-diameter hole in the middle; see also Supplementary Fig. 1) and UV light Norland Optical Adhesive (NOA) curing. Use tweezers to connect the tip–tubing assembly to a 27-gauge needle and then screw the needle to the syringe. Fill the whole system with HFE-7500.

(ii) Prepare a second syringe for the reagent assay sample as described in Step 32A(i).

(iii) Prepare a syringe for the continuous phase by putting a 23-gauge needle on the syringe; then use tweezers to connect it to 0.3-mm-diameter PTFE microtubing and fill the whole assembly with HFE-7500 oil containing 2% (wt/wt) fluorinated surfactant.

▲ CRITICAL STEP Care should be taken to remove any air bubbles. If air bubbles are present, hold the syringe in a vertical position with the opening facing upward and push the plunger until the air is completely removed.

(iv) Mount the syringes on the syringe pumps and prime the assembly by applying a flow rate of 1,000 µl/h for the reagent syringes to remove air bubbles from the assembly (syringes from Step 32A(i, ii), reagent syringes) for about 30 s. The station is ready for loading of the samples.

(v) Take antibody-coated beads from Step 31A(lvi), pipette 10 µl of antibody-coated beads into a new 1.5-ml tube and then sonicate for 3 min at room temperature.

? TROUBLESHOOTING

(vi) Prepare the assay reagents for syringe 1 as follows: Add PE anti TNF-α antibody to a final concentration of 0.4 µg/ml (from 20-µg/ml stock) and antibody-coated beads at a concentration of 0.2 mg/ml (from 5-mg/ml stock) in cell buffer 1. For each calibration point, prepare ~25 µl.

▲ CRITICAL STEP Centrifuge the PE anti TNF-α antibody at 10,000 g for 5 min at 4 °C to remove aggregates.

(vii) For syringe 2, prepare dilutions of recombinant TNF-α to desired concentration in cell buffer 1 (0–100 nM).

(B) **Detection of murine IgG using a droplet microfluidic assay** ● Timing **2 h**

▲ CRITICAL Following this protocol and using the respective dilutions will lead to a beadline capacity of ~60 nM within each droplet and ~1,200 nanoparticles per droplet. Each concentration counts as an experiment, so prepare a sufficient volume of beads (in Step 31B(i–ix)).

(i) Follow Step 32A(i–iv).

(ii) Take the functionalized nanoparticles (25 µl of nanoparticles per experiment) from Step 31B(ix). Add the following reagents to the beads (all final concentrations): 150 nM AffiniPure $F(ab')_2$ fragment rabbit anti-mouse IgG, Fcγ fragment specific, 60 nM Zenon Alexa Fluor 488 Anti-Mouse IgG2b; and 60 nM fluorescent antigen of interest.

▲ CRITICAL STEP Centrifuge the fluorescent proteins at 10,000*g* for 5 min at 4 °C to remove large aggregates before using the solution. For the preparation of fluorescent molecules, refer to Boxes 1 and 2.

▲ CRITICAL STEP Over prolonged storage time, the beads will slowly sediment. Resuspended every hour with a pipette.

? TROUBLESHOOTING

(iii) For calibration, prepare a dilution series of murine calibration IgG in cell buffer 2. Start with 200 nM and divide the concentration by a factor of 2 down to 6.25 nM. Do not forget to prepare IgG cell buffer 2 with no added IgG as a blank measure.

▲ CRITICAL STEP Before calibrating your own antibodies, we recommend using murine control isotypes (such as those supplied by Thermo Fisher Scientific) for a general calibration of the system.

Generation of droplets ● Timing 15 min

33 Place the pipette tips of the sample syringes in a sample tube (Supplementary Fig. 1), one in the desired concentration of the calibration solution and the other in the final bead solution, and aspirate 25 µl at a 2,000 µl/h rate of the bead and the calibration solutions.

34 Connect the syringes to the corresponding inlet holes of the microfluidic device and connect the device outlet to waste with 0.30-mm-diameter PTFE microtubing.

35 Set the flow rates for the aqueous solutions and oil phase at 100 µl/h and then start the pumps to inject fluids into the chip. Once the droplet production is stabilized and the fluid leaves the outlet (~8 to 10 µl of volume used), increase the flow rate of oil to 300 µl/h to generate droplets of 50-pL volume.

36 To collect the droplets, connect the microfluidic device outlet to the incubation chamber (from Step 28A or 28B, according the application) using a new piece of 0.3-mm-diameter PTFE microtubing. Attach the tubing to the nanoport of the observation chamber with a MicroTight fitting adaptor. Fill the chamber with droplets (visible as a gray, homogeneous and turbid layer). Once filled, remove the tubing and fluid remaining in the nanoports and close the chamber with the caps.
▲ **CRITICAL STEP** The loading of the cells in a pipette tip (rather than a syringe), the encapsulation process and the chamber filling should take <5 min and is typically performed at room temperature. If longer operating time is required, density-matching agents (such as OptiPrep, Percoll and methyl cellulose) can be added to the cell buffer. However, cells can also be cooled to 4 °C to reduce secretion before encapsulation in droplets, if required—although this may slow their secretion rate, at least initially—after encapsulating and changing to the desired temperature for secretion measurements. To cool, a small hole is drilled or punched into the bottom of a 2-ml Eppendorf tube. The pipette tip is then introduced into the chip through the Eppendorf tube and glued in place. The volume between the pipette tip and the tube is filled with ice water during droplet loading.
▲ **CRITICAL STEP** Clean the outside surfaces of the incubation chamber with isopropanol and water before filling. Apply Scotch tape to the glass chamber to remove residual dust particles.
? TROUBLESHOOTING

37 Transfer the filled chamber to the microscope for image acquisition (Steps 38–45) and repeat Steps 33–45 for all other calibration solutions.
? TROUBLESHOOTING

Image acquisition ● Timing 45 min

38 Start the epifluorescence microscope and set the heat at 37 °C at least 30 min before starting acquisition.
▲ **CRITICAL STEP** Care should be taken so that the experiment is performed at 37 °C because the biological responses are optimal at this temperature. Imaging at room–temperature will result in a reduced cellular secretion rate and may also interfere with cellular secretion per se.

39 Open the acquisition software and set up the image acquisition program. We typically perform quality controls of the droplets by manually acquiring a few images with a 10× objective (bright-field (20 ms), DAPI (300 ms to 1 s), GFP (200–500 ms), CY3 (200ms to 1 s), and CY5 (200–500 ms). Once acquisition exposure times have been defined, they should not be modified for a defined assay if a calibration curve is performed.
▲ **CRITICAL STEP** Clean the objective before imaging.
▲ **CRITICAL STEP** Exposure times will depend on the exact setup used and can be adapted depending on the assay and reagents used. Fix exposure time to ensure absence of saturation and optimal fluorescence quantification.

40 Position the chamber on the microscope stage insert (Supplementary Fig. 2).
- *Chamber for sepsis application*. When one magnet is attached to the chamber, place the chamber so that the magnet is located on the left when facing the microscope; the beadline is located in the left part of each droplet on the acquired bright-field image.
- *Chamber for IgG application*. Position the chamber on the microscope stage insert and place the magnet holder above it so that the magnet is located in the front and back of the stage. Check the position with bright-field microscopy: The beadline should be located in the top or bottom part of each droplet, span >2/3 of the droplet diameters and be vertical or horizontal in orientation.

41 Start the PFS.
▲ **CRITICAL STEP** This step is critical because it allows maintaining the focus at different locations of the incubation chamber over time (corrects for potential drift of focus over time and scan).

42 Use the bright-field channel and adjust the focus manually so that the contours of droplets and beadlines appear as dark objects on the bright-field image (to facilitate automated detection).
▲ **CRITICAL STEP** This step is critical because sharp focus is needed for optimal signals, as well as automated analysis.

43 Position the objective in the middle of the incubation chamber and then set up the imaging matrix to be acquired using the microscope software.
▲ CRITICAL STEP Do not acquire images close to the magnet. Before imaging and after installation of the chamber, wait for 2–5 min for the temperature to equilibrate to reduce droplet movement due to this difference.

44 After the completion of the experiment, save the images as ND2 files and switch off the microscope and the heating system.
? TROUBLESHOOTING

45 At this step of the protocol, perform quality control of the images. Potential issues are undesired movement of droplets during acquisition, aggregation of nanobeads, irregular distribution of beads within the droplets, presence of clusters, more than one layer of droplet within the imaging microfluidic chamber (see the 'Troubleshooting' section).
- *Quality control movement*. Open the images in the software, choose the bright-field image and focus on a single field of view. Activate the time-lapse function; the software will show you the images over time. If no movement is visible (<1/10 of the diameter can be tolerated), repeat this step for two other fields of view. A small fraction of droplets (<2%) might rearrange their positions; these need to be removed manually or tracked.
- *Quality control droplets and layers*. Similarly, the presence of droplets with varying diameter (>95% should be similar in diameter), as well as the presence of multiple layers of droplets, can be easily assessed by looking at the bright-field images. In the former case, some data might be usable; in the latter there is no other way than to repeat the experiment. We recommend repeating the experiment in both cases.
- *Aggregation of nanobeads*. Aggregates of nanoparticles can also be seen in the bright-field image. Usually these are potato-shaped clusters that show bright fluorescence. Therefore, also check the empty droplets, where no secreting cell is present. These can lead to false-positive events (see also the 'Troubleshooting' section).
- *Irregular distribution of beads within the droplets*. This phenomenon can be checked in the bright-field view and the fluorescence channels. Often, this issue is accompanied by droplets showing different levels of fluorescence (brighter/darker droplets) and speaks of problems during encapsulation. We recommend repeating the experiment in this case.
- *Presence of clusters*. The presence of cell clusters can also be checked in the bright-field view. A relatively easy control is to calculate the cell/droplet ratio and compare the distribution of individual cells/droplets, with the expected distribution following a Poisson distribution. If no other issues occur, these data might still be usable, but they are usually accompanied by an uneven distribution of dyes and antibodies as well (see above), making their analysis difficult.
? TROUBLESHOOTING

Cell measurements

46 The protocol can be used for a variety of different cells. The first application uses human monocytes from healthy donors and septic shock patients (option A), whereas the second application uses murine IgG-secreting cells that were extracted from the spleen and bone marrow of immunized animals (option B). Other tissues or cell types can also be analyzed. However, cell preparation should be rapid and gentle, generating a singularized suspension of un-clumped cells.

(A) **Sepsis application** ● Timing **5.5 h**

(i) Start the laminar flow hood for cell culture 15 min before starting cell extraction.

(ii) Use an EasySep Direct Human Monocyte Isolation Kit to isolate highly pure $CD14^+$ monocytes from human whole blood.
▲ CRITICAL STEP This protocol enables the isolation of live cells without using density-gradient centrifugation or cell lysis buffers. For optimal recovery of monocyte isolation, use EDTA as an anticoagulant to collect blood samples. Follow the EasySep Kit instructions to isolate monocytes from 3 ml of human blood.

(iii) After the end of the EasySep protocol, pipette 7 µl to count the cells using FastRead 102 slides.

(iv) Add 20 µl of the fluorescently labeled anti-CD14 antibody stock to the cells to stain monocytes.

(v) Incubate for 12 min at room temperature in the dark.

(vi) Centrifuge the cells at 2,800*g* for 7 min at room temperature and carefully remove the plasma from the cell pellet.

▲ CRITICAL STEP Carefully discard the supernatant. Do not disturb the cell pellet.

▲ CRITICAL STEP If residual red blood cells are present in the isolated cells, resuspend the pellet in PBS for one additional separation step. The red blood cells can be also removed by lysis with ammonium chloride solution.

(vii) Take antibody-coated beads from Step 31A(lvi), pipette 10 µl of antibody-coated beads into a new 1.5-ml tube and then sonicate for 3 min at room temperature.

? TROUBLESHOOTING

(viii) Resuspend at 10^6 monocytes from Step 46A(vi) per 100 µl of cell culture buffer containing 20 mM HEPES. This is the final cell sample.

(ix) To a separate volume of cell buffer 1, add the following assay reagents (all final concentrations): 0.5 µg/ml LPS, 0.4 µg/ml PE anti TNF-α, 0.2 mg/ml antibody-coated nanoparticles, NucView and MitoView probes at 2×.

▲ CRITICAL STEP LPS is omitted for the control experiment. Centrifuge the PE anti-TNF-α antibody at 10,000*g* for 5 min at 4 °C to remove aggregates.

? TROUBLESHOOTING

(x) Prepare the syringes for the cell sample and reagent assay samples as described in Step 32A(i).

(xi) Prepare a syringe for the continuous phase as described in Step 32A(iii).

▲ CRITICAL STEP Care should be taken to avoid air bubble formation. If air bubbles are formed, hold the syringe in a vertical position with the opening facing upward and push the plunger until the air bubbles are completely removed.

(xii) Mount the syringes on the NeMESYS pump and prime the assembly by applying a flow rate of 1,000 µl/h for ~50 µl. Discard the fluid. The station is ready for loading of samples.

(xiii) Place the pipette tips in the separate sample tubes containing the cell sample and the assay reagents (Supplementary Fig. 1) and aspirate 50 µl at a 2,000 µl/h rate.

(xiv) Connect pipette tips to the corresponding inlet holes of the microfluidic device and connect the device outlet to waste with 0.30-mm-diameter PTFE microtubing.

(xv) Set the flow rates of the aqueous solutions and oil phase at 100 µl/h and then start the pumps to inject fluids into the chip. Once droplet production is stabilized (1–2 min), increase the flow rate of oil to 300 µl/h to generate droplets of 50-pL volume.

? TROUBLESHOOTING

(xvi) To collect the droplets, connect the microfluidic device outlet to the incubation chamber with new PTFE microtubing. Fill the chamber with droplets (visible as a gray, homogeneous and turbid layer). Once filled, remove the tubing and fluid remaining in the nanoports and close the chamber with the caps.

(xvii) Immediately proceed to image acquisition as described in Steps 38–45. In Step 39, use the following image acquisition settings: BF (20 ms), DAPI (1 s), GFP (500 ms), CY3 (1 s), and CY5 (500 ms) images and a 10× objective. 75 fields (25 × 3) every 30 min over 3 h (7 time points). If a calibration curve is used for secretion, the same acquisition exposure times defined at Step 39 need to be used.

▲ CRITICAL STEP If the chamber is not clean, wipe the surfaces with ethanol or dust them off using compressed air or Scotch tape.

? TROUBLESHOOTING

(B) **Murine IgG-measurement application** ● Timing **2 h**

(i) Prepare spleen, bone marrow or other organs of interest according to the established protocol of your laboratory or follow reference[38]. Note that the cells should be well suspended and present as individual cells in order to proceed and obtain optimal results.

▲ CRITICAL STEP In our experience, different protocols will result in slightly different secretion rates. Harsh conditions and protocols, that is, strong shear forces or chemical stress, may result in decreased secretion rates.

(ii) Count cells in the suspension and centrifuge the volume equivalent of 2 million cells. Resuspend the cells in PBS.

(iii) Add 1 µl/ml of CellTrace Violet (5 mM stock in DMSO); mix by pipetting and incubate the cells for 15–30 min at 37 °C. Dilute the cells afterward in cell buffer 2 to quench the reaction.

(iv) Take the beads from the assay in Step 32B(ii).

(v) Centrifuge the labeled cells at 400*g* for 5 min at room temperature and carefully remove the supernatant from the cell pellet. Resuspend gently but fully in 150 µl of cell buffer 2. Proceed immediately to cell assay and encapsulation.

▲ CRITICAL STEP The concentration of cells is optimized to result in the optimum amount of droplets containing an individual cell. Work quickly and proceed directly to the encapsulation because the cells will continue to secrete in bulk.

▲ CRITICAL STEP The cellular density is quite high in this volume. For a short time (<1–2 h), the cells can be stored on ice. Longer storage will result in a substantial decrease in IgG secretion and cellular response.

(vi) Prepare the syringes for the cell sample, bead solution and continuous phase as described in Step 32A(i and iii).

(vii) Mount the syringes on the NeMESYS pumps and prime the assembly by flowing 50 µl of solutions with a flow rate of 1,000 µl/h. Clean the pipette tips of oil by wiping them with tissue. No air bubbles should be visible in the pipette tips.

(viii) Place the syringes with added pipette tips into the sample tubes (Supplementary Fig. 1), one in the prepared cell suspension and the other in the final bead solution, and aspirate 50 µl at a 2,000 µl/h rate for the beads and the calibration dilution.

(ix) Connect the syringes to the corresponding inlet holes of the microfluidic device.

(x) Set the flow rates of aqueous solutions and oil phase at 100 µl/h and then start the pumps to inject fluids into the chip. Once the droplet production is stabilized, increase the flow rate of oil to 300 µl/h to generate droplets of 50-pL volume.

? TROUBLESHOOTING

(xi) To collect the droplets, connect the microfluidic device outlet to the incubation chamber with 0.30-mm-diameter PTFE microtubing.

(xii) Immediately proceed to image the droplets as described in Steps 38–45. In Step 39, use the following image acquisition settings: DAPI (300 ms), GFP (200 ms), CY3 (200 ms), CY5 (200 ms) and BF (20 ms) with a 10× objective and 100 fields of view (10 × 10) every 10 min over 60 min (7 time points). If a calibration curve is used for secretion, the same acquisition exposure times defined at Step 39 need to be used.

Automated image processing

47 For image processing of data obtained for the sepsis application, follow option A. For image processing of data obtained for the murine IgG measurements, follow option B.

(A) **Sepsis application** ● Timing **4 h**

(i) Extract images from ND2 files (Nikon file format) and save them in TIFF format: 5,250 images are extracted per experiment, including both the kinetics acquired with and without LPS.

(ii) Open the input_parameter.txt file and set the required parameters (e.g., path to the folder containing the input images, vector of field numbers, vector of time points, various display and saving parameters).

(iii) Run the standalone MATLAB application DropCell.exe.

▲ CRITICAL STEP Image data without LPS and with LPS must be located in different folders and must be analyzed separately. Make sure five TIFF images are present per field in the input data folder, named according to the required naming rules. Make sure (by checking a few bright-field images) that the beadline is always located in the left-hand-part of the droplets and that its length is lower than one-third of the droplet's diameter.

▲ CRITICAL STEP Modify the input_parameters.txt file carefully, observing format instructions. Do not open Excel while running DropCell.exe.

▲ CRITICAL STEP Check the suitability of the analysis parameters on a few fields and time points before running the analysis of an entire experiment.

(iv) Process the output STATdrops_sorting_YYYY-M-D_H-M-S.xlsx file obtained after the execution of DropCell.exe is completed. The Single-cell sheet focuses on single-cell-containing droplets. CY3 relocalization fluorescence signal (signal-to-noise ratio) per droplet and time point are given in the column 't**_Signal_CY3'. 'trackingfail_time', 'rodfail_time', 'death_time' and 'phagocytosis_time' columns are used, when setting appropriate filters, to select the droplets of interest (single, live, and non-endocytic cells through the entire kinetics).

(B) **Murine IgG measurements** ● Timing **3–4 h**

(i) Extract images from ND2 files (Nikon file format) and save them in a TIFF format (Nikon file format; 1 TIFF file per time point) and transfer the images to the workstation for calculation.

(ii) Open the MATLAB script and run the provided script (analyze.m, https://github.com/LCMD-ESPCI/dropmap-analyzer).

(iii) A window will pop up. Within the first line, define the channels where you want to measure the beadline (as channel index within the file; see also the readme file on GitHub). Next, define the bright-field channel; this will be used to detect the droplets. Define the number of time points and the average droplet radius in pixels. If you follow the protocol described herein, 25 pixels is a good a starting point for 50-pL droplets.
▲ **CRITICAL STEP** The algorithm is sensitive to the droplet diameter you define. You might need to increase or decrease the diameter if you change certain variables in the protocol.

(iv) The output files are Microsoft Excel files wherein each channel is a separate sheet, sorted by columns for beadline signal over time, average droplet signal over time and ratio of the two values over time. In addition, MATLAB files containing the images of the recognized droplets are saved by index.

(v) Use the calibration curve to convert ratios to concentration of analyte.
▲ **CRITICAL STEP** Be sure to take the correct curve for the proper channel.

(vi) Refer to Box 2 for the extraction of parameters. Sort and select droplets of interest in a separate sheet and combine the information.

(vii) After analysis, check the selected droplets with the verify function (verify.m) to exclude false-positive events. The verify program will show the droplets to verify their content. It will ask for a list of indices to check.
▲ **CRITICAL STEP** Control the selected events for false-positive events (dead cells or others) and exclude those from further analysis.

Chamber cleaning after experiments ● Timing 5 min

▲ **CRITICAL** If desired, the chambers can be used over 4–8 weeks for multiple experiments. After the measurements, the droplets should be removed from the chamber before storage.

48 Repeat Step 18 but fill the syringe with HFE-7500 oil. Connect the tubing to the nanoport using MicroTight fitting adaptors.

49 Flush the chamber with 1 ml HFE-7500 oil to remove droplets.

50 Close the nanoport chamber with caps and keep it in a dust-free environment.

Troubleshooting

Troubleshooting advice can be found in Table 2.

Table 2 | Troubleshooting table

Step	Problem	Possible reason	Solution
11	Cracking in the inlets or outlets during punching	Blunt or clogged punch	Use a new punch
		Insufficient mixing of PDMS and curing agent	Vigorously mix PDMS and curing agent to achieve a homogeneous mixture of the two components. Do not cure for prolonged times (>24 h)
14	Microfluidic device delaminates during surface treatment	Plasma protocol was not optimal	Check and adapt the parameters of your plasma procedure
		Glass slides were not sufficiently clean	Use clean glass slides; wash the glass slides with acetone, isopropanol and Milli-Q water. Repeat if necessary
15, 18–22, 46A (xvii), 46B(x)	No droplet formation during experiments	Collapsed microfluidic channels	Reduce force when sealing PDMS slab to glass slide
		Aqueous solutions wet the microfluidics channels	Repeat the surface treatment of the device
		Dirt present within the microfluidic assembly	Observe microfluidic chips after fabrication for crystal formation or the presence of dust particles
		Absence of sufficient concentration of surfactant	Use HFE-7500 with an added 2.0% (wt/wt) fluorosurfactant

Table continued

Table 2 (continued)

Step	Problem	Possible reason	Solution
28A(i–vii)	Microfluidic chamber leakage	Inefficient sealing	Use clean glass slides and work clean
			Increase the duration of incubation during Step 28A(vi)
			Make sure that the nanoports are well sealed with UV glue
31A(i), 31B(i)	Aggregation of nanobeads	Presence of air within the chamber	Remove air bubbles before acquiring images
		Microfluidic chamber is leaking	Check Steps 27 and 28A(i–vii)
		Aggregation is inherent to the beads	Increase sonication time
		Long-term storage of beads	It should be noted that extended sonication time can heat the nanoparticles, denaturing the functionalized antibodies. Ice can be added to the bath to limit nanoparticle overheating
32A(v), 32B(ii), 37, 46A(vii)	Irregular distribution of beads within the droplets, presence of clusters	Beads aggregate during coupling	COOH beads: increase sonication time
			Streptavidin-beads: bead-crosslinking due to over-biotinylated immobilization reagent. After Step 31B (iii), add 10 μM biotin before collecting the beads. Incubate for 5–10 min before collection
		Aggregation occurred during storage of coupled beads	Reversible formation of clusters is normal but should be reversible by pipetting or sonication
36, 45, 46A(xvii)	Observed movement of droplets during acquisition	Droplet coalescence occurs	Increase the concentration of surfactant
		Chamber height is bigger than the droplet diameter	Fabricate a chamber with proper height (<90% of droplet diameter). Make sure that the height of the chamber is optimal for your droplet volume
36, 46A(xvii), 46B(x)	More than one layer of droplet is formed	The thickness of chamber is bigger than the droplet diameter	Reduce the thickness of the chamber or increase the volume of the droplets
39–45	Rapid decrease of droplet and beadline fluorescence	Photobleaching	Optimally, reduce illumination intensity and/or exposure time. Otherwise, reduce the total number of time points
44; Box 4, step 18	Failure to detect the target molecule	Insufficient coupling efficiency	Adapt concentration or incubation times. Use a fluorescent antibody to establish optimal labeling of beads. Additionally, in our experience, fluorescent analyte (TNF-A488, or Ig-A488) helps greatly to analyze problems
		Positive calibration samples did not result in in fluorescence relocation	Make sure that the protein solutions used as positive calibration controls are not degraded
			Make sure of calculations of concentrations
			Make sure that no free dye is present in the fluorescent detection antibody solution. Remove free dye by centrifugation with molecular cutoff spin columns
		No cellular secretion of target molecule detectable	Use an alternative method to confirm cellular secretion of the analyte (ELISA; ELISPOT; flow cytometry with brefeldin A or similar)
45, 46A(ix)	Cells are not fluorescent	Cells are necrotic	Discard these cells from the analyses
			Use a probe that can detect necrotic cells
		Live and dead cell staining protocol is not optimal	Optimize the concentration of live/dead probes
46A(xv), 46B(x)	Cell aggregates and clumps are present in the microfluidic chip during encapsulation	Nucleic acids are released from dead cells	Add benzonase to cell suspension for DNA and RNA removal

Timing

Steps 1–22, droplet maker fabrication: 4 h
Steps 23–27, observation chamber fabrication: 10 min plus 5 min per slide
Step 28A, microfluidic chamber assembly—sepsis application: 3–5 h
Step 28B, microfluidic chamber assembly—murine IgG application: 1.5 h
Steps 29 & 30, surface treatment of the chamber: 10 min
Step 31A, boronic acid coupling: 20 h (4 h hands-on)

Step 31B, biotin–streptavidin coupling: 2 h
Step 32A, detection of TNF-α with droplet assay: 2 h
Step 32B, detection of murine IgG with droplet assay: 2 h
Steps 33–37, droplet generation: 15 min
Steps 38–45, image acquisition: 1 h
Step 46A, sepsis application: 5.5 h
Step 46B, murine IgG measurement application: 2 h
Step 47A, sepsis application: 4 h
Step 47B, murine IgG measurements: 3–4 h
Steps 48–50, chamber cleaning after experiments: 5 min
Box 4, microtiter plate assay: 3 h

Anticipated results

The DropMap system is a flexible platform for high-throughput single-cell phenotypic analysis that is particularly well adapted to the characterization of immune responses. The protocol can be modified to enable the single-cell quantitative analysis of a wide range of cell-surface markers and secreted molecules expressed by a range of different cell types, simultaneously with other cellular characteristics such as endocytosis and viability. The development described here expands its potential from the analysis of humoral to cell-mediated and innate immune responses.

The ability of DropMap to simultaneously measure secretion rates and affinities of antibodies from thousands of single B cells makes it a powerful tool for studying humoral immune responses[38], for example, following vaccination[72] or infection. Furthermore, the large datasets from these single-cell experiments can easily be adapted as training sets for deep learning/artificial intelligence strategies, and allow in silico modeling and simulation of the immune responses following vaccination. Such strategies could ultimately contribute to the reduction or replacement of animal experiments.

The system is also well adapted to study the role of T cells in both humoral and cell-mediated immune responses. Given their constitutive role in immune surveillance, aberrant T cell functions are linked to autoimmune diseases as well as to carcinogenesis and defective protection against pathogen infections[73,74]. In this protocol, we demonstrate our approach by integrating the measurement of secretion of a range of murine and human cytokines produced by T cells identified using a fluorescent anti-CD3 antibody. For example, we show here the measurement of the secretion rates of TNF-α, IFN-γ, IL-2 and IL-4 from human T cells (Fig. 5, limits of detection (LODs) of 10.4 nM, 0.6 nM, 0.5 nM and 0.2 nM for human IL-2, IL-4, TNF-α and IFN-γ, respectively). Distribution of secretion rates is shown for ex vivo–stimulated and unstimulated peripheral blood mononuclear cells (PBMCs; stimulated with PMA/ionomycin).

Interestingly, stimulation with phorbol 12-myristate 13-acetate (PMA)/ionomycin did not significantly affect the median secretion rates of TNF-α ($N = 4$ independent experiments, unstimulated 25 ± 13 molecules/s; stimulated 28 ± 15 molecules/s, P value = 0.77, mean ± s.d. of the median values for the independent experiments, two-tailed unpaired t-test) but significantly increased the percentage of secreting T cells by ~8-fold (from 2.5 ± 0.6% to 17 ± 11%, mean ± s.d., $P = 0.05$, two-tailed unpaired t-test, Fig. 5a). By contrast, upon stimulation, there were significant increases in the frequency and secretion rates of T cells secreting INF-γ ($N = 4$ independent experiments, 1 ± 1% versus 19 ± 5%, $P = 0.004$; and 4.7 ± 2.8 molecules/s versus 22.5 ± 12.8 molecules/s, $P < 0.05$, both mean ± s.d. of the median values for the independent experiments, two-tailed unpaired t-test, Fig. 5b), a pro-inflammatory cytokine signature for the Th1 T cell subset that is critical for fighting viral infections[75–77]. The average median rate of IL-2 secretion by T cells ($N = 3$ independent experiments, 0 ± 1.1% versus 24 ± 10%, $P = 0.01$, mean ± s.d.; and 43 ± 5 molecules/s versus 73 ± 18 molecules/s, $P = 0.05$, mean ± s.d. of the median values for the independent experiments, two-tailed unpaired t-test, Fig. 5c) was equivalent with or without stimulation, whereas a 10-fold increase of the frequency of IL2-secreting cells was found in the stimulated sample. A low frequency (<2%) and low (but measurable) secretion rates ($N = 3$ independent experiments, 0.6 ± 0.7% versus 1.7 ± 0.7%, non-significant in a two-tailed unpaired t-test, mean ± s.d.; and 4.4 ± 3.2 molecules/s versus 4.2 ± 2.7 molecules/s, non-significant in a two-tailed unpaired t-test, mean ± standard deviation of the median values for the independent experiments, Fig. 5d) were observed for IL-4-secreting cells in both samples. The detection of IL-4 at low expression levels in a small subset of cells nicely illustrates the advantages of DropMap and its use for the analysis of cytokine secretion by T cells at the single-cell level. This opens up new opportunities to improve our fundamental understanding of immune responses, for

example, to study T cell plasticity[78], which may lead to the development of novel therapeutic strategies. It is also a promising approach for clinical single-cell immuno-monitoring for patient stratification and personalized medicine.

We also extend the DropMap system to analyze innate immune responses and to monitor the dysfunction of monocytes from septic shock patients (Table 1). Septic shock is the most severe form of sepsis[79,80]. Sepsis is a complex clinical syndrome characterized by an early dysregulated inflammatory response. This response, triggered by the recognition of microbial patterns by receptors such as Toll-like receptors (TLRs), is often followed by a post-infective complex immune dysfunction combining innate and adaptive immune defects, such as monocyte dysfunction, which is characterized by decreased TNF-α production and release[81].

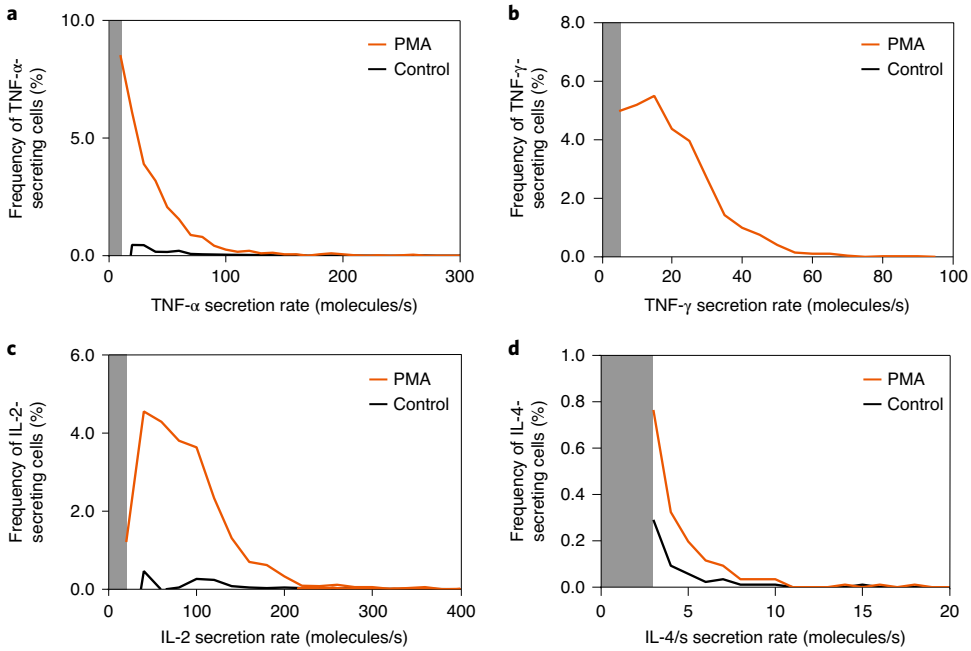

Fig. 5 | Analysis of cytokine secretion from human single T cells. a–d, Distribution of the frequencies of TNF-α (**a**), IFN-γ (**b**), IL-2 (**c**) and IL-4-secreting (**d**) T cells (identified using a fluorescent FITC-conjugated anti-CD3 antibody) in PMA/ionomycin-stimulated human PBMCs (orange) and non-stimulated PBMCs (black). **a** and **b** depict 4,515 stimulated and 7,525 non-stimulated PBMCs. **c** and **d** depict 8,640 and 8,606 individually assayed stimulated and non-stimulated cells, respectively. The data represent a single experiment. No or only little secretion was found in the population of $CD3^-$ cells. Gray bars represent the part of the distribution that could not be analyzed because of the LOD of the assays (see also Boxes 1 and 2).

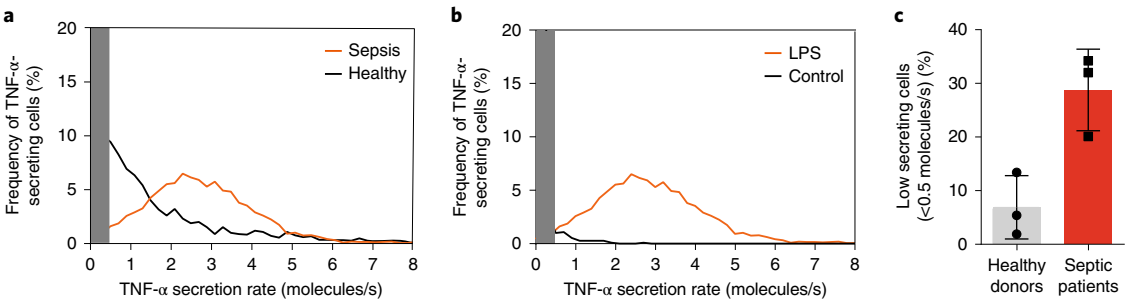

Fig. 6 | Analysis of TNF-α secretion from human single monocytes of a healthy donor and a septic shock patient. a, Distribution of the frequencies of TNF-α-secreting monocytes upon LPS stimulation of a healthy donor (black line, 3,008 cells) and a septic shock patient (orange line, 2,473 cells). **b**, Distribution of the frequencies of TNF-α-secreting monocytes upon LPS stimulation (orange line, 3,008 cells) and non-stimulated cells (black line, 1,099 cells) of a healthy donor. Poorly secreting cells exhibit a TNF-α secretion rate <0.5 molecules per s. The data represent a single experiment. Gray bars represent the part of the distribution that could not be analyzed because of the LOD (TNF-α secretion rate <0.5 molecules per s) of the assay (see also Boxes 1 and 2). **c**, Percentage of poorly secreting monocytes of septic patients ($N = 3$ patients, black squares, 29 ± 8%, mean ± s.d. for the independent experiments) and healthy donors ($N = 3$ donors, black circles, 6 ± 6%, mean ± s.d. for the independent experiments). Error bars show standard deviation.

Table 3 | Analysis of single monocytes from healthy donors and septic shock patients using DropMap

	Cell no.	Dead cells (%)	Secretion rate (molecules/s)	Cells with low secretion rates (%)	Endocytic cells (%)
Healthy donor 1	2,215	0.6	3.6	1.8	31
Healthy donor 2	3,008	0.5	2.5	5.3	31
Healthy donor 3	4,495	0.4	1.4	13.3	26
Septic patient 1	2,473	1.6	0.9	34.1	61
Septic patient 2	1,122	3.8	1.9	20.0	69
Septic patient 3	3,077	0.4	1.0	31.9	39

Number of LPS stimulated cells per experiment, percentage of dead cells, secretion rate (molecules/s), percentage of cells with low secretion rates, and the percentage of endocytic cells of 3 healthy donors and 3 septic shock patients. Dead monocytes were determined by measuring caspase-3 activity in droplets. Endocytic activity was assessed by counting the number of single monocytes that bind to or internalize the magnetic beadline.

To evaluate the potential of DropMap in this context, we first controlled its ability to maintain a viable primary human monocyte population in a confined environment over the course of an experiment with and without pro-inflammatory LPS. For all experiments, only a small fraction of cells showed apoptotic activity (0.49 ± 0.09% for $N = 3$ healthy donors and 1.94 ± 1.75% for $N = 3$ septic patients, mean ± s.d. for the independent experiments, Table 3), demonstrating that the encapsulation process allows functional analysis.

Deactivation of circulating monocytes is currently viewed as the soundest indicator of sepsis-induced immunosuppression[79,80], and reduced production rate of TNF-α by monocytes in bulk, upon in vitro stimulation by LPS, is used a biomarker to monitor sepsis-induced immunosuppression in intensive care unit patients[81]. However, no standardized tool is currently available in routine practice to assess the functionality of septic patients' immune systems. Here, we show that the DropMap system can be used to assess the TNF-α secretion rate of single monocytes from septic shock patients in response to LPS stimulation.

In agreement with previous studies[22], single-cell DropMap measurements revealed lower rates of TNF-α secretion by monocytes upon LPS activation in septic shock patients ($N = 3$ patients, 1.3 ± 0.5 molecules/s, mean ± s.d. of the median values for the independent experiments) compared with those of healthy donors ($N = 3$ donors, 2.5 ± 1.1 molecules/s, mean ± s.d. of the median values for the independent experiments, Fig. 6a and Table 3). Without LPS, only a small fraction (3%) of monocytes secrete TNF-α ($N = 1$ donor, $n = 32$ monocytes, 0.9 ± 0.4 molecules/s, mean ± s.d.), demonstrating that cell activation is specifically trigged by LPS stimulation (Fig. 6b). Interestingly, the frequency of monocytes, having a TNF-α secretion rate <0.5 molecules per s (i.e., below the LOD of the bioassay), was higher in septic shock patients ($N = 3$ patients, 29 ± 8%, mean ± s.d. for the independent experiments) than in healthy donors ($N = 3$ donors, 6 ± 6%, mean ± s.d. for the independent experiments). These differences were at the limit of statistical significance ($P = 0.05$ with one-sided Mann-Whitney test) (Fig. 6c).

Furthermore, monocytes from sepsis patients have been reported to exhibit higher endocytic activity compared with those of healthy donors[82]. The uptake of nanobeads is usually used as a readout for functional phenotyping of cell endocytosis[83–85]. We thus used the DropMap platform to monitor over time the uptake of nanobeads (endocytic activity) by monocytes. As expected, we observed differences in nanobead uptake between cells of healthy donors ($N = 3$ donors, 29 ± 3%, mean ± s.d. for the independent experiments) and septic shock patients ($N = 3$ patients, 56 ± 15%, mean ± s.d. for the independent experiments, Table 3). These differences were at the limit of statistical significance ($P = 0.05$ with one-sided Mann-Whitney test). This result should be taken cautiously given the small number of samples. Overall, these results exemplify the potential application and added value of the DropMap technology in clinical studies.

The DropMap system is a valuable tool for monitoring cell responses and probing heterogeneity with single-cell resolution that can be applied in the field of immuno-monitoring, and beyond, to address a large panel of fundamental research or clinical questions. It is robust and simple, and it can be easily adapted to measure other cell types, in healthy and diseased states, and to measure other secreted molecules (such as microRNAs, other cytokines, chemokines and enzymes).

Reporting Summary

Further information on research design is available in the Nature Research Reporting Summary linked to this article.

Data availability

The datasets generated during and/or analyzed during the current study are not publicly available due to confidentiality and contractual obligations toward industrial partners of the project in which the data were generated but are available from the corresponding author upon reasonable request.

Code availability

The DropMap MATLAB script is available from the GitHub repository, https://github.com/LCMD-ESPCI/dropmap-analyzer. MATLAB scripts illustrating the main functions performed by the DropCell.exe MATLAB application are available from GitHub repository https://github.com/bioaster/dropcell.git. The installation file for the DropCell.exe MATLAB application, as well as an image dataset that supports/illustrates the findings of this study, are available in the figshare repository, with the identifiers https://figshare.com/articles/DropCell_exe_installer/11336663/1 and https://figshare.com/articles/dropcell_image_data_set/11342426/1, respectively.

References

1. Lawson, D. A., Kessenbrock, K., Davis, R. T., Pervolarakis, N. & Werb, Z. Tumour heterogeneity and metastasis at single-cell resolution. *Nat. Cell Biol.* **20**, 1349–1360 (2018).
2. Potter, S. S. Single-cell RNA sequencing for the study of development, physiology and disease. *Nat. Rev. Nephrol.* **14**, 479–492 (2018).
3. Stuart, T. & Satija, R. Integrative single-cell analysis. *Nat. Rev. Genet.* **20**, 257–272 (2019).
4. Svensson, V., Vento-Tormo, R. & Teichmann, S. A. Exponential scaling of single-cell RNA-seq in the past decade. *Nat. Protoc.* **13**, 599–604 (2018).
5. Zhang, X. et al. Comparative analysis of droplet-based ultra-high-throughput single-cell RNA-Seq systems. *Mol. Cell* **73**, 130–142.e5 (2018).
6. Battle, A. et al. Genomic variation. Impact of regulatory variation from RNA to protein. *Science* **347**, 664–667 (2015).
7. Peterson, V. M. et al. Multiplexed quantification of proteins and transcripts in single cells. *Nat. Biotechnol.* **35**, 936–939 (2017).
8. Shapiro, H. M. *Practical Flow Cytometry* (Wiley-Liss, 2003).
9. Bendall, S. C. et al. Single-cell mass cytometry of differential immune and drug responses across a human hematopoietic continuum. *Science* **332**, 687–696 (2011).
10. Becattini, S. et al. Functional heterogeneity of human memory CD4(+) T cell clones primed by pathogens or vaccines. *Science* **347**, 400–406 (2015).
11. Betts, M. R. et al. Sensitive and viable identification of antigen-specific CD8+ T cells by a flow cytometric assay for degranulation. *J. Immunol. Methods* **281**, 65–78 (2003).
12. Han, G., Spitzer, M. H., Bendall, S. C., Fantl, W. J. & Nolan, G. P. Metal-isotope-tagged monoclonal antibodies for high-dimensional mass cytometry. *Nat. Protoc.* **13**, 2121–2148 (2018).
13. Korin, B., Dubovik, T. & Rolls, A. Mass cytometry analysis of immune cells in the brain. *Nat. Protoc.* **13**, 377–391 (2018).
14. Stoeckius, M. et al. Simultaneous epitope and transcriptome measurement in single cells. *Nat. Methods* **14**, 865–868 (2017).
15. Shahi, P., Kim, S. C., Haliburton, J. R., Gartner, Z. J. & Abate, A. R. Abseq: ultrahigh-throughput single cell protein profiling with droplet microfluidic barcoding. *Sci. Rep.* **7**, 44447 (2017).
16. Czerkinsky, C. C., Nilsson, L. A., Nygren, H., Ouchterlony, O. & Tarkowski, A. A solid-phase enzyme-linked immunospot (ELISPOT) assay for enumeration of specific antibody-secreting cells. *J. Immunol. Methods* **65**, 109–121 (1983).
17. Kouwenhoven, M. et al. Enzyme-linked immunospot assays provide a sensitive tool for detection of cytokine secretion by monocytes. *Clin. Diagn. Lab. Immunol.* **8**, 1248–1257 (2001).
18. Schultes, B. C. & Whiteside, T. L. Monitoring of immune responses to CA125 with an IFN-gamma ELISPOT assay. *J. Immunol. Methods* **279**, 1–15 (2003).
19. Mogensen, T. H. Pathogen recognition and inflammatory signaling in innate immune defenses. *Clin. Microbiol. Rev.* **22**, 240–273 (2009).
20. Garcia-Cordero, J. L., Nembrini, C., Stano, A., Hubbell, J. A. & Maerkl, S. J. A high-throughput nanoimmunoassay chip applied to large-scale vaccine adjuvant screening. *Integr. Biol. (Camb.)* **5**, 650–658 (2013).
21. Han, Q. et al. Polyfunctional responses by human T cells result from sequential release of cytokines. *Proc. Natl Acad. Sci. USA* **109**, 1607–1612 (2012).

22. Han, Q., Bradshaw, E. M., Nilsson, B., Hafler, D. A. & Love, J. C. Multidimensional analysis of the frequencies and rates of cytokine secretion from single cells by quantitative microengraving. *Lab Chip* **10**, 1391–1400 (2010).
23. Shirasaki, Y. et al. Real-time single-cell imaging of protein secretion. *Sci. Rep.* **4**, 4736 (2014).
24. Son, K. J. et al. Microfluidic compartments with sensing microbeads for dynamic monitoring of cytokine and exosome release from single cells. *Analyst* **141**, 679–688 (2016).
25. Varadarajan, N. et al. A high-throughput single-cell analysis of human CD8(+) T cell functions reveals discordance for cytokine secretion and cytolysis. *J. Clin. Invest.* **121**, 4322–4331 (2011).
26. Xue, Q. et al. Single-cell multiplexed cytokine profiling of CD19 CAR-T cells reveals a diverse landscape of polyfunctional antigen-specific response. *J. ImmunoTher. Cancer* **5**, 85 (2017).
27. Xue, Q. et al. Analysis of single-cell cytokine secretion reveals a role for paracrine signaling in coordinating macrophage responses to TLR4 stimulation. *Sci. Signal.* **8**, ra59 (2015).
28. Yamanaka, Y. J. et al. Cellular barcodes for efficiently profiling single-cell secretory responses by micro-engraving. *Anal. Chem.* **84**, 10531–10536 (2012).
29. Seah, Y. F. S., Hu, H. & Merten, C. A. Microfluidic single-cell technology in immunology and antibody screening. *Mol. Asp. Med.* **59**, 47–61 (2018).
30. Love, J., Ronan, J., Grotenbreg, G., Van Der Veen, A. & Ploegh, H. A microengraving method for rapid selection of single cells producing antigen-specific antibodies. *Nat. Biotechnol.* **24**, 703–707 (2006).
31. Jin, A. et al. Rapid isolation of antigen-specific antibody-secreting cells using a chip-based immunospot array. *Nat. Protoc.* **6**, 668–676 (2011).
32. Köster, S. et al. Drop-based microfluidic devices for encapsulation of single cells. *Lab Chip* **8**, 1110–1115 (2008).
33. Clausell-Tormos, J. et al. Droplet-based microfluidic platforms for the encapsulation and screening of mammalian cells and multicellular organisms. *Chem. Biol.* **15**, 427–437 (2008).
34. El Debs, B., Utharala, R., Balyasnikova, I. V., Griffiths, A. D. & Merten, C. A. Functional single-cell hybridoma screening using droplet-based microfluidics. *Proc. Natl Acad. Sci.* **109**, 11570–11575 (2012).
35. Mazutis, L. et al. Single-cell analysis and sorting using droplet-based microfluidics. *Nat. Protoc.* **8**, 870–891 (2013).
36. Shembekar, N., Hu, H., Eustace, D. & Merten, C. A. Single-cell droplet microfluidic screening for antibodies specifically binding to target cells. *Cell Rep.* **22**, 2206–2215 (2018).
37. Chokkalingam, V. et al. Probing cellular heterogeneity in cytokine-secreting immune cells using droplet-based microfluidics. *Lab Chip* **13**, 4740–4744 (2013).
38. Eyer, K. et al. Single-cell deep phenotyping of IgG-secreting cells for high-resolution immune monitoring. *Nat. Biotechnol.* **35**, 977–982 (2017).
39. Jorgolli, M. et al. Nanoscale integration of single cell biologics discovery processes using optofluidic manipulation and monitoring. *Biotechnol. Bioeng.* **116**, 2393–2411 (2019).
40. Mocciaro, A. et al. Light-activated cell identification and sorting (LACIS) for selection of edited clones on a nanofluidic device. *Commun. Biol.* **1**, 41 (2018).
41. Winters, A. et al. Rapid single B cell antibody discovery using nanopens and structured light. *mAbs* **11**, 1025–1035 (2019).
42. Konry, T., Dominguez-Villar, M., Baecher-Allan, C., Hafler, D. A. & Yarmush, M. L. Droplet-based microfluidic platforms for single T cell secretion analysis of IL-10 cytokine. *Biosens. Bioelectron.* **26**, 2707–2710 (2011).
43. Qiu, L. et al. A membrane-anchored aptamer sensor for probing IFNγ secretion by single cells. *Chem. Commun. (Camb.)* **53**, 8066–8069 (2017).
44. Segaliny, A. I. et al. Functional TCR T cell screening using single-cell droplet microfluidics. *Lab Chip* **18**, 3733–3749 (2018).
45. Gérard, A. et al. High-throughput single-cell activity-based screening and sequencing of antibodies using droplet microfluidics. *Nat. Biotechnol.* **38**, 715–721 (2020).
46. Armbruster, D. A. & Pry, T. Limit of blank, limit of detection and limit of quantitation. *Clin. Biochem. Rev.* **29**(Suppl 1), S49–S52 (2008).
47. Duffy, D. C., McDonald, J. C., Schueller, O. J. & Whitesides, G. M. Rapid prototyping of microfluidic systems in poly(dimethylsiloxane). *Anal. Chem.* **70**, 4974–4984 (1998).
48. Anna, S. L., Bontoux, N. & Stone, H. A. Formation of dispersions using "flow focusing" in microchannels. *Appl. Phys. Lett.* **82**, 364–366 (2003).
49. Akhtar, M., van den Driesche, S., Bödecker, A. & Vellekoop, M. J. Long-term storage of droplets on a chip by Parylene AF4 coating of channels. *Sens. Actuators B Chem.* **255**, 3576–3584 (2018).
50. Di Carlo, D., Aghdam, N. & Lee, L. P. Single-cell enzyme concentrations, kinetics, and inhibition analysis using high-density hydrodynamic cell isolation arrays. *Anal. Chem.* **78**, 4925–4930 (2006).
51. Jin, S. H., Jeong, H. H., Lee, B., Lee, S. S. & Lee, C. S. A programmable microfluidic static droplet array for droplet generation, transportation, fusion, storage, and retrieval. *Lab Chip* **15**, 3677–3686 (2015).
52. Liu, C., Liu, J., Gao, D., Ding, M. & Lin, J. M. Fabrication of microwell arrays based on two-dimensional ordered polystyrene microspheres for high-throughput single-cell analysis. *Anal. Chem.* **82**, 9418–9424 (2010).
53. Ochsner, M. et al. Micro-well arrays for 3D shape control and high resolution analysis of single cells. *Lab Chip* **7**, 1074–1077 (2007).

54. Schmitz, C. H., Rowat, A. C., Koster, S. & Weitz, D. A. Dropspots: a picoliter array in a microfluidic device. *Lab Chip* **9**, 44–49 (2009).
55. Duval, F., van Beek, T. A. & Zuilhof, H. Key steps towards the oriented immobilization of antibodies using boronic acids. *Analyst* **140**, 6467–6472 (2015).
56. Kumar, S., Aaron, J. & Sokolov, K. Directional conjugation of antibodies to nanoparticles for synthesis of multiplexed optical contrast agents with both delivery and targeting moieties. *Nat. Protoc.* **3**, 314–320 (2008).
57. Saha, B., Evers, T. H. & Prins, M. W. How antibody surface coverage on nanoparticles determines the activity and kinetics of antigen capturing for biosensing. *Anal. Chem.* **86**, 8158–8166 (2014).
58. Saha, B., Songe, P., Evers, T. H. & Prins, M. W. J. The influence of covalent immobilization conditions on antibody accessibility on nanoparticles. *Analyst* **142**, 4247–4256 (2017).
59. Sivaram, A. J., Wardiana, A., Howard, C. B., Mahler, S. M. & Thurecht, K. J. Recent Advances in the generation of antibody-nanomaterial conjugates. *Adv. Healthc. Mater.* **7**, 1700607 (2018).
60. Welch, N. G., Scoble, J. A., Muir, B. W. & Pigram, P. J. Orientation and characterization of immobilized antibodies for improved immunoassays (review). *Biointerphases* **12**, 02d301 (2017).
61. Dhadge, V. L., Hussain, A., Azevedo, A. M., Aires-Barros, R. & Roque, A. C. Boronic acid-modified magnetic materials for antibody purification. *J. R. Soc. Interface* **11**, 20130875 (2014).
62. Lin, P. C. et al. Fabrication of oriented antibody-conjugated magnetic nanoprobes and their immunoaffinity application. *Anal. Chem.* **81**, 8774–8782 (2009).
63. Wang, X., Xia, N. & Liu, L. Boronic acid-based approach for separation and immobilization of glycoproteins and its application in sensing. *Int. J. Mol. Sci.* **14**, 20890–20912 (2013).
64. Wagner, O. et al. Biocompatible fluorinated polyglycerols for droplet microfluidics as an alternative to PEG-based copolymer surfactants. *Lab Chip* **16**, 65–69 (2016).
65. Williamson, J. D. & Cox, P. Use of a new buffer in the culture of animal cells. *J. Gen. Virol.* **2**, 309–312 (1968).
66. Lowe, K. C. Perfluorochemical respiratory gas carriers: benefits to cell culture systems. *J. Fluor. Chem.* **118**, 19–26 (2002).
67. Holtze, C. et al. Biocompatible surfactants for water-in-fluorocarbon emulsions. *Lab Chip* **8**, 1632–1639 (2008).
68. Mazutis, L. & Griffiths, A. D. Selective droplet coalescence using microfluidic systems. *Lab Chip* **12**, 1800–1806 (2012).
69. Scott, R. L. The solubility of fluorocarbons. *J. Am. Chem. Soc.* **70**, 4090–4093 (1948).
70. Simons, J. H. & Linevsky, M. J. The solubility of organic solids in fluorocarbon derivatives. *J. Am. Chem. Soc.* **74**, 4750–4751 (1952).
71. Qin, D., Xia, Y. & Whitesides, G. M. Soft lithography for micro- and nanoscale patterning. *Nat. Protoc.* **5**, 491–502 (2010).
72. Eyer, K. et al. The quantitative assessment of the secreted IgG repertoire after recall to evaluate the quality of immunizations. *J. Immunol.* https://doi.org/10.4049/jimmunol.2000112 (2020).
73. Raphael, I., Nalawade, S., Eagar, T. N. & Forsthuber, T. G. T cell subsets and their signature cytokines in autoimmune and inflammatory diseases. *Cytokine* **74**, 5–17 (2015).
74. Tanaka, A. & Sakaguchi, S. Regulatory T cells in cancer immunotherapy. *Cell. Res.* **27**, 109–118 (2017).
75. Kang, S., Brown, H. M. & Hwang, S. Direct antiviral mechanisms of interferon-gamma. *Immune Netw.* **18**, e33 (2018).
76. Mosmann, T. R., Cherwinski, H., Bond, M. W., Giedlin, M. A. & Coffman, R. L. Two types of murine helper T cell clone. I. Definition according to profiles of lymphokine activities and secreted proteins. *J. Immunol.* **136**, 2348–2357 (1986).
77. Wheelock, E. F. Interferon-like virus-inhibitor induced in human leukocytes by phytohemagglutinin. *Science* **149**, 310–311 (1965).
78. DuPage, M. & Bluestone, J. A. Harnessing the plasticity of CD4(+) T cells to treat immune-mediated disease. *Nat. Rev. Immunol.* **16**, 149–163 (2016).
79. Cecconi, M., Evans, L., Levy, M. & Rhodes, A. Sepsis and septic shock. *Lancet* **392**, 75–87 (2018).
80. Gyawali, B., Ramakrishna, K. & Dhamoon, A. S. Sepsis: the evolution in definition, pathophysiology, and management. *SAGE Open Med.* **7**, 2050312119835043 (2019).
81. Monneret, G. et al. Novel approach in monocyte intracellular TNF measurement: application to sepsis-induced immune alterations. *Shock* **47**, 318–322 (2017).
82. Shalova, I. N. et al. Human monocytes undergo functional re-programming during sepsis mediated by hypoxia-inducible factor-1alpha. *Immunity* **42**, 484–498 (2015).
83. Kumar, P., Pai, K., Pandey, H. P. & Sundar, S. Study on pinocytosis by monocytes from visceral leishmaniasis patients. *Curr. Sci.* **83**, 631–633 (2002).
84. Luciani, N., Gazeau, F. & Wilhelm, C. Reactivity of the monocyte/macrophage system to superparamagnetic anionic nanoparticles. *J. Mater. Chem.* **19**, 6373–6380 (2009).
85. Robert, D. et al. Cell sorting by endocytotic capacity in a microfluidic magnetophoresis device. *Lab Chip* **11**, 1902–1910 (2011).

Acknowledgements

We acknowledge the support of the REALISM study group: HCL: A. Boibieux, J. Davidson, L. Fayolle-Pivot, J. Gatel, C. Genin, A. Gregoire, A. Lepape, A.-C. Lukaszewicz, G. Marcotte, Marie Matray, D. Maucort-Boulch, N. Panel, T. Rimmele, H. Vallin; bioMérieux: S. Blein, K. Brengel-Pesce, E. Cerrato, V. Cheynet, E. Gallet-Gorius, A. Guichard, C. Jourdan, N. Koenig, F. Mallet, B. Meunier,

M. Mommert, G. Oriol, C. Schrevel, O. Tabone, J. Yugueros Marcos; Bioaster: J. Becker, F. Bequet, F. Brajon, B. Canard, M. Collus, N. Garcon, I. Gorse, F. Lavocat, K. Louis, J. Moriniere, Y. Mouscaz, L. Noailles, M. Perret, F. Reynier, C. Riffaud, M.-L. Rol, N. Sapay; Sanofi: C. Carre, A. de Monfort, K. Florin, L. Fraisse, I. Fugier, M. L'Azou, S. Payrard, A. Peleraux, L. Quemeneur; ESPCI: S. Toetsch; GSK: T. Ashton, P.J. Gough, S.B. Berger, D. Gardiner, A. MacNamara, A. Raychaudhuri, R. Smylie, L. Tan, C. Tipple. This research project received funding from the French Government through the "Investissement d'Avenir" program (grant no. ANR-10-AIRT-03) and from bioMérieux. K.E. acknowledges generous funding from the 'The Branco Weiss Fellowship – Society in Science' and received funding from the European Research Council (ERC) under the European Union's Horizon 2020 research and innovation programme (grant agreement no. 80336). This work also received support from "Institut Pierre-Gilles de Gennes" (laboratoire d'excellence, "Investissements d'Avenir" programs ANR-10-IDEX-0001-02 PSL, ANR-10- EQPX-34 and ANR-10-LABX-31). This work was also supported by BPIFrance under the framework "Programme d'Investissements d'Avenir" (CELLIGO Project). The authors thank the healthy donors and the septic patients who volunteered to donate peripheral blood for these experiments. We also thank M.-N. Unheheuer, H. Laude and B.L. Perlaza for access to the BioResources platform (ICAReB). We thank F. Pène, who collected clinical samples from septic shock patients at the medical intensive care unit of Cochin Hospital (CPP17-053a / 2017-A01134-49). We thank F. Porcheray for critical reading of the manuscript. We further acknowledge the help of P. Canales Herrerias and P. Bruhns for their helpful discussion and supervision of the immunization of mice.

Author contributions

Y.B., K.E., M.R. and N.A. performed and optimized the experiments described in this protocol, S.D. and G.C. provided the respective MATLAB scripts for data analysis; C.C and T.T. provided the statistical tools. M.M. optimized the boronic acid nanobead functionalization protocol. C.V. and J. Baudry managed the optical bench setup. J.-F.L. supplied the septic clinical samples. K.E., J. Bibette, J. Baudry and A.D.G. developed the DropMap technology[38] and contributed to the early-stage definition of the new technology. Y.B. and C.V. extended the DropMap technology to measure low cytokine secretion profiles and to overcome limitations of cell endocytic activity. G.M., A.P. and J.T. designed and set up the clinical study involving sepsis and matched-control patients. A.T., C.G., P.L., V.M., F.V., P.C. and I.A.G. supervised the work, participated to the design of technical experiments and of the clinical study, and actively contributed in writing different sections of the manuscript. Y.B., S.D. and C.V. analyzed the data for the sepsis application, and Y.B., K.E., J. Baudry, A.D.G. and C.V. wrote the manuscript. All authors edited and proofread the paper.

Competing interests

Some of the authors (J. Baudry, J. Bibette, A.D.G., Y.B. & C.V.) are inventors on patent applications based on certain ideas described in this paper and may receive financial compensation via their employers' rewards-to-inventors schemes.

Additional information

Supplementary information is available for this paper at https://doi.org/10.1038/s41596-020-0354-0.

Correspondence and requests for materials should be addressed to J.B., A.D.G. or C.V.

Reprints and permissions information is available at www.nature.com/reprints.

Publisher's note Springer Nature remains neutral with regard to jurisdictional claims in published maps and institutional affiliations.

Received: 27 December 2018; Accepted: 6 May 2020;
Published online: 12 August 2020

Related links

Key references using this protocol

Eyer, K., et al. *Nat. Biotechnol.* **35**, 977–982 (2017): https://www.nature.com/articles/nbt.3964

Rybczynska, M., et al. **38**, 5337–5342 (2020): https://doi.org/10.1016/j.vaccine.2020.05.066

nature research

Corresponding author(s): Christophe Védrine, Andrew Griffiths, Jean Baudry

Last updated by author(s): Apr 28, 2020

Reporting Summary

Nature Research wishes to improve the reproducibility of the work that we publish. This form provides structure for consistency and transparency in reporting. For further information on Nature Research policies, see Authors & Referees and the Editorial Policy Checklist.

Statistics

For all statistical analyses, confirm that the following items are present in the figure legend, table legend, main text, or Methods section.

n/a	Confirmed	
☐	☒	The exact sample size (*n*) for each experimental group/condition, given as a discrete number and unit of measurement
☐	☒	A statement on whether measurements were taken from distinct samples or whether the same sample was measured repeatedly
☐	☒	The statistical test(s) used AND whether they are one- or two-sided *Only common tests should be described solely by name; describe more complex techniques in the Methods section.*
☐	☒	A description of all covariates tested
☒	☐	A description of any assumptions or corrections, such as tests of normality and adjustment for multiple comparisons
☐	☒	A full description of the statistical parameters including central tendency (e.g. means) or other basic estimates (e.g. regression coefficient) AND variation (e.g. standard deviation) or associated estimates of uncertainty (e.g. confidence intervals)
☐	☒	For null hypothesis testing, the test statistic (e.g. *F*, *t*, *r*) with confidence intervals, effect sizes, degrees of freedom and *P* value noted *Give P values as exact values whenever suitable.*
☒	☐	For Bayesian analysis, information on the choice of priors and Markov chain Monte Carlo settings
☒	☐	For hierarchical and complex designs, identification of the appropriate level for tests and full reporting of outcomes
☒	☐	Estimates of effect sizes (e.g. Cohen's *d*, Pearson's *r*), indicating how they were calculated

Our web collection on statistics for biologists contains articles on many of the points above.

Software and code

Policy information about availability of computer code

Data collection	NIS-Elements (Version 4.50)
Data analysis	Matlab (R2019a version 9.6, Image processing toolbox and VLFeat open source library), Custom DropMap Matlab scripts available from GitHub repositories. Application/alternative 1: SEPSIS • Installation file for DropCell.exe Matlab application is available in figshare repository, https://doi.org/10.6084/m9.figshare.11336663.v1 • Matlab scripts illustrating the main functions performed by the DropCell.exe Matlab application are available from GitHub repository, https://github.com/bioaster/dropcell.git Application/alternative 2: Murine Ig-measurements • DropMap Matlab script is available from GitHub repository, https://github.com/LCMD-ESPCI/dropmap-analyzer

For manuscripts utilizing custom algorithms or software that are central to the research but not yet described in published literature, software must be made available to editors/reviewers. We strongly encourage code deposition in a community repository (e.g. GitHub). See the Nature Research guidelines for submitting code & software for further information.

Data

Policy information about availability of data

All manuscripts must include a data availability statement. This statement should provide the following information, where applicable:

- Accession codes, unique identifiers, or web links for publicly available datasets
- A list of figures that have associated raw data
- A description of any restrictions on data availability

Application/alternative 1: SEPSIS
• An image data set that support/illustrate the findings of this study are available in figshare repository, https://figshare.com/articles/dropcell_image_data_set/11342426

Application/alternative 2: Murine Ig-measurements
• An image data set that support/illustrate the findings of this study are available in https://github.com/LCMD-ESPCI/dropmap-analyzer

Field-specific reporting

Please select the one below that is the best fit for your research. If you are not sure, read the appropriate sections before making your selection.

☒ Life sciences ☐ Behavioural & social sciences ☐ Ecological, evolutionary & environmental sciences

For a reference copy of the document with all sections, see nature.com/documents/nr-reporting-summary-flat.pdf

Life sciences study design

All studies must disclose on these points even when the disclosure is negative.

Sample size	Different experiments (on murine B cells, human T cells from PBMCs of healthy donors, human monocytes from whole blood of healthy donors or septic shock patients) were analyzed to illustrate the potential of the single-cell analysis technology. For each experiment, 3 to 4 different samples, each taken from different mice or human donors, were independently tested. The number of single-cells analyzed in each sample ranged from 1000 to 8600.
Data exclusions	Data from droplets containing >1 cell were excluded from the analyses (as the aim of the study was to measure phenotypes of single-cells)
Replication	During the method development steps, duplicate experiments (same sample studied) were performed to ensure that results were reproducible at cell population level.
Randomization	No method of randomization was chosen. Fresh blood samples from septic shock patients were processed as soon as they were available. Dedicated appointments were set up for healthy donors.
Blinding	No blinding was performed.

Reporting for specific materials, systems and methods

We require information from authors about some types of materials, experimental systems and methods used in many studies. Here, indicate whether each material, system or method listed is relevant to your study. If you are not sure if a list item applies to your research, read the appropriate section before selecting a response.

Materials & experimental systems

n/a	Involved in the study
☐	☒ Antibodies
☒	☐ Eukaryotic cell lines
☒	☐ Palaeontology
☐	☒ Animals and other organisms
☐	☒ Human research participants
☐	☒ Clinical data

Methods

n/a	Involved in the study
☒	☐ ChIP-seq
☒	☐ Flow cytometry
☒	☐ MRI-based neuroimaging

Antibodies

Antibodies used

Anti-CD14, blue violet conjugate (Clone TÜK4) (Miltenyi Biotec, cat. no. 130-094-364, Batch 5171130409).
Capture anti-TNF-α antibody (Antibody TNF5) (Mabtech, cat. no 3510-6-1000, Batch 16, non-biotinylated).
Detection PE-anti-TNF-α antibody Clone: cA2 (Miltenyi Biotec, specific production without azid, cat. no. 120-014-229 equivalent to cat. no. 130-120-489 containing azid, Batch 5160222264).

CaptureSelect™ Biotin Anti-LC-kappa (Murine) Conjugate (ThermoFisher Scientific, cat. no. 7103152100). Lot number
AffiniPure F(ab')$_2$ Fragment Rabbit Anti-Mouse IgG, Fcγ fragment specific (Jackson ImmunoResearch, cat. no. 315-606-0466). Lot number

IFN gamma Monoclonal Antibody (MD-1), eBioscience™ - Cat. 14-7317-85, LOT 4295084, biotinylated in house
IFN gamma Monoclonal Antibody (clone 4S.B3), APC conjugate, eBioscience - Cat. 17-7219-82; LOT 4281150
TNF alpha Monoclonal Antibody (MAb1), eBioscience™ - Cat. 14-7348-85, LOT E05529-432, biotinylated in house
TNF alpha Monoclonal Antibody (MAb11), PE conjugate, eBioscience™ - Cat. 12-7349-81, LOT 4290466
IL-2 Polyclonal Antibody, Biotin, eBioscience™ - Cat. 13-7028-81; LOT 4307122 and 2049448
IL-2 rabbit anti-human, PeproTech, cat. 500-P22, LOT 0204CY12RB, labelled in house with Alexa 555
IL-4 Monoclonal Antibody (MP4-25D2), Biotin conjugate, eBioscience™ - Cat. 13-7048-81; LOT 1963900
IL-4 Monoclonal Antibody (8D4-8), APC conjugate, eBioscience™ - Cat. 17-7049-81, LOT 4275080

Alexa Fluor® 647 anti-human CD3, clone HIT3a Cat. RT2101610

Validation

Anti-CD14, blue violet conjugate:
https://www.miltenyibiotec.com/FR-en/products/macs-flow-cytometry/antibodies/primary-antibodies/cd14-antibodies-human-tuk4-1-50.html

Capture anti-TNF-α antibody:
https://www.mabtech.com/sites/default/files/datasheets/3510-6-1000.pdf

Detection PE-anti-TNF-α antibody:
https://www.miltenyibiotec.com/FR-en/products/macs-flow-cytometry/antibodies/primary-antibodies/anti-tnf-a-antibodies-human-ca2-1-50.html#pe:for-100-tests

CaptureSelect™ Biotin Anti-LC-kappa (Murine) Conjugate (ThermoFisher Scientific, cat. no. 7103152100). Lot#160707-02
https://www.thermofisher.com/order/catalog/product/7103152100#/7103152100

Alexa Fluor® 647 AffiniPure F(ab')$_2$ Fragment Rabbit Anti-Mouse IgG, Fcγ fragment specific (Jackson ImmunoResearch, cat. no. 315-606-0466). Lot#103179
https://www.jacksonimmuno.com/catalog/products/315-606-046

IFN gamma Monoclonal Antibody (MD-1), eBioscience™ - Cat. 14-7317-85, LOT 4295084, biotinylated in house
https://www.thermofisher.com/antibody/product/IFN-gamma-Antibody-clone-MD-1-Monoclonal/14-7317-85

IFN gamma Monoclonal Antibody (clone 4S.B3), APC conjugate, eBioscience - Cat. 17-7219-82; LOT 4281150
https://www.thermofisher.com/antibody/product/IFN-gamma-Antibody-clone-4S-B3-Monoclonal/17-7319-82

TNF alpha Monoclonal Antibody (MAb1), eBioscience™ - Cat. 14-7348-85, LOT E05529-432, biotinylated in house
https://www.thermofisher.com/antibody/product/TNF-alpha-Antibody-clone-MAb1-Monoclonal/14-7348-81

TNF alpha Monoclonal Antibody (MAb11), PE conjugate, eBioscience™ - Cat. 12-7349-81, LOT 4290466
https://www.thermofisher.com/antibody/product/TNF-alpha-Antibody-clone-MAb11-Monoclonal/12-7349-82

IL-2 Polyclonal Antibody, Biotin, eBioscience™ - Cat. 13-7028-81; LOT 4307122 and 2049448
https://www.thermofisher.com/antibody/product/IL-2-Antibody-Polyclonal/13-7028-81

IL-2 rabbit anti-human, PeproTech, cat. 500-P22, LOT 0204CY12RB, labelled in house with Alexa 555
https://www.peprotech.com/gb/search?q=human%20IL-2&cat=Antibodies&subcat=Antigen+Affinity+Purified+Polyclonal+Antibodies

IL-4 Monoclonal Antibody (MP4-25D2), Biotin conjugate, eBioscience™ - Cat. 13-7048-81; LOT 1963900
https://www.thermofisher.com/antibody/product/IL-4-Antibody-clone-MP4-25D2-Monoclonal/14-7048-81

IL-4 Monoclonal Antibody (8D4-8), APC conjugate, eBioscience™ - Cat. 17-7049-81, LOT 4275080
https://www.thermofisher.com/antibody/product/IL-4-Antibody-clone-8D4-8-Monoclonal/17-7049-42

Animals and other organisms

Policy information about studies involving animals; ARRIVE guidelines recommended for reporting animal research

Laboratory animals

Mus musculus, BALB/cJRj, females, age 8-10 weeks at the start of the immunization, supplied by Janvier Laboratories

Wild animals

Provide details on animals observed in or captured in the field; report species, sex and age where possible. Describe how animals were caught and transported and what happened to captive animals after the study (if killed, explain why and describe method; if released, say where and when) OR state that the study did not involve wild animals.

Field-collected samples

For laboratory work with field-collected samples, describe all relevant parameters such as housing, maintenance, temperature, photoperiod and end-of-experiment protocol OR state that the study did not involve samples collected from the field.

Ethics oversight

Experiments using mice have been validated by the CETEA ethics committee number 89 (Institut Pasteur, Paris, France) under #2013-0103, and by the french Ministery of Research under agreement #00513.02, and are part of larger scientific study.

Note that full information on the approval of the study protocol must also be provided in the manuscript.

Human research participants

Policy information about studies involving human research participants

Population characteristics

We included 3 septic shock patients with a sec ratio (F/M)=2:1, a mean age of 70 y/o and a mean SOFA score of 7.3.

Recruitment

Septic shock samples and negative controls
Samples from septic shock patients were obtained from the prospective cohort MICROFLU-SEPSIS. Patients were included in the medical intensive care unit of Cochin hospital.
The age and health status of healthy donors and their blood were provided by the Investigation Clinique et Acces aux Resources

	Biologiques (ICAReB) platform (Dr Marie-Noelle Ungeheuer, Centre de Recherche Translationnelle, Institut Pasteur, Paris, France). Blood samples: Peripheral Human blood was also collected from healthy patients at the "Etablissement Français du Sang". Donors were recruited after a medical selection process complying with French regulations, and they gave their informed consent to participation in the study.
Ethics oversight	Prospective cohort MICROFLU-SEPSIS: French Ethical Committee CPP Sud Ouest et Outre Mer 4 (registration number 2017-A01134-49). Healthy donor cohort as part of the DIAGMICOLL or CoSImmGEn (N° CORC: 2008-16 and 201-06) protocol, which has been approved by the French Ethical Committee (CPP).

Note that full information on the approval of the study protocol must also be provided in the manuscript.

Clinical data

Policy information about clinical studies

All manuscripts should comply with the ICMJE guidelines for publication of clinical research and a completed CONSORT checklist must be included with all submissions.

Clinical trial registration	French Ethical Committee CPP Sud Ouest et Outre Mer 4 (registration number 2017-A01134-49)
Study protocol	Whereas we provide clinical data for three patients in our study, we cannot provide a ClinicalTrial number since the french law does not require to declare non-interventionnal observationnal data to a multinational database. However, according to guidelines, our protocol (named "MicroFlu Sepsis ») is declared and recorded into the french database and written informed consent of participation were obtained in all three patients.
Data collection	We performed venous puncture in the three septic patients in the intensive care unit of Cochin
Outcomes	No clinical outcome was measured